buildings

MDPI

Article

Bending Analysis of Stepped Rectangular Plates Resting on an Elastic Half-Space Foundation

Jian Wu [1], Jinpeng Zhang [1] and Xue Li [2,*]

[1] Shaanxi Key Laboratory of Safety and Durability of Concrete Structures, Xijing University, Xi'an 710123, China; wujian2085@126.com (J.W.); jpzh1999@163.com (J.Z.)
[2] College of Science, Xi'an University of Architecture and Technology, Xi'an 710055, China
* Correspondence: lixue891225@126.com

Abstract: In this paper, the bending behavior of rectangular plates with stepped thickness resting on an elastic half-space foundation is investigated through an analytic method. Combined with the bending theory of the rectangular thin and moderately thick plate, the stepped rectangular plate is divided into upper and lower plates, and the Fourier series is used to obtain the analytical solution of the deflection of the plate and the interaction force between the plate and foundation. The influence of the elastic modulus of the plate, plate theory, and the dimension of the plate on the deflection of the stepped rectangular plate is also discussed. The results show that the analytical solution is basically the same as the existing research results, and it is also verified by the analysis results of the models established by ABAQUS software. The deflection at the center of the stepped rectangular plate increases with the increase of the elastic modulus of the upper plate and the decrease of the side length of the upper plate, while the plate theory has little effect on the deflection of the plate. This method not only overcomes some of the disadvantages of numerical methods but also eliminates the assumptions of the Winkler foundation model and the two-parameter foundation model, thus obtaining a more reasonable and accurate bending performance of the stepped rectangular plate resting on the elastic half-space foundation.

Keywords: stepped rectangular plate; thin plate theory; moderately thick plate theory; static; bending performance

Citation: Wu, J.; Zhang, J.; Li, X. Bending Analysis of Stepped Rectangular Plates Resting on an Elastic Half-Space Foundation. *Buildings* **2023**, *13*, 1671. https://doi.org/10.3390/buildings13071671

Academic Editors: Jaroslaw Rybak, Andrea Segalini and Marian Drusa

Received: 26 May 2023
Revised: 22 June 2023
Accepted: 27 June 2023
Published: 29 June 2023

1. Introduction

Plate-foundation systems have become a research hotspot in civil engineering. Much practical engineering, such as foundation plates in civil engineering [1], piezoelectric laminated plates in electronic engineering [2], and pavement plates supporting the traffic load [3], can be simplified into a mechanical model for analysis [4]. In order to provide necessary parameters for the model of these structures, two methods are usually used. One is to provide accurate models for various types of plates and the interaction between the plate and foundation. The other one is to develop a numerical analysis method and computer codes for the solution of practical engineering problems.

In the past few centuries, much work has been done to develop simplified models of foundations to promote applications in engineering design. The Winkler foundation model, in which the foundation is assumed as a single layer of vertical springs, was first proposed in the 1860s [5]. However, the accuracy of this model cannot be guaranteed in the analysis of nonlinear conditions of the foundation. Thus, the linear spring is replaced by a nonlinear type of model to overcome this shortage [6]; this model can be used in static analysis [7] and dynamic analysis [8], but it still cannot accurately analyze the frictional foundation due to the reason that the analysis model of the Winkler foundation eliminates the interfacial shear stress. Thus, researchers have proposed two-parameter and multi-parameter models to solve this problem. Compared to the Winkler model, the two-parameter Pasternak

foundation model has shear and vertical stiffness with nonlinear properties, which is helpful to improve the efficiency of the model, without resulting in significant loss of the accuracy of calculation results [9,10]. In addition, the three-parameter model [11] and the frictional model [7] were also proposed by researchers. Although the refinement of the parameters could improve the applicability of the foundation model, the increase of the number of the parameters will enhance the complication of the calculation process.

The plate theory also plays an important role in the simulation of numerical models and the structure design of the plate-foundation system. The Kirchhoff plate theory [12] and the Mindlin plate theory [13] are the two types of classical plate theories widely used in the simulation of plate foundations. The in-plane deformation of the plate is assumed to be linearly changed in the classical plate theories, and these theories could only be used in the analysis of thin and moderately thick plates. Many studies have been carried out using the classical plate theories. Özdemir [14,15] investigated the static performance, free vibration properties, and transient response of thick plates resting on the elastic Winkler foundation with the finite element method. Farida et al. [16] presented the efficient analysis of plates resting on an elastic half-space foundation using the boundary element method. Ragba et al. [17] used convolution and indirect meshless techniques to obtain the vibration performance of irregular composite plates on the linear and parabolic Winkler foundations. Ferreira et al. [18] investigated the free vibration problem of the plate resting on the Winkler foundation using the wavelet collocation method. Investigations of the Kirchhoff plate on foundations are also reported in the literature. Yue et al. [19] analyzed the influence of soil heterogeneity on the bending of a circular thin plate using two modified Vlasov foundation models. Mohammadimehr et al. [20] obtained the buckling and free vibration response of functionally graded materials resting on a Pasternak foundation. To promote the development of the plate theory, higher-order shear deformation theory and quasi-3D theory have attracted the attention of researchers in recent years, and these theories take into account the nonlinear deformation of the plates. Singh et al. [21] used the stress-function Galerkin method to investigate the dynamic response of a sandwich functionally graded plate resting on a Pasternak elastic foundation. Huang et al. [22] studied the nonlinear dynamic performance of functionally graded material plates using an improved perturbation technique. Rachid et al. [23] and Vu et al. [24] used different quasi-3D theories to analyze the static response of the plate. Kumar et al. [25] investigated the vibration performance of stepped FGM plates using the dynamic stiffness method.

Based on the foundation models and the different plate theories, analytical models can be used to obtain the accurate solution for the plate-foundation systems. Compared with the literature using numerical methods, analytical methods are not commonly used due to the difficulties in the partial differential equations and various boundary conditions [26]. Yan [27] introduced the usage of the Fourier series in the analysis of the bending, stability, and vibration of the plate. The deflection of the plate was expressed as a double Fourier series, and the various boundary conditions were used to obtain the analytical solution of the plate resting on the Winkler foundation. Wang [28] used the method mentioned in [27] to investigate the interaction and deflection of the thin plate resting on the elastic half-space foundation. The foundation models eliminated the assumptions of the Winkler foundation to overcome the shortages of the Winkler model to obtain a more accurate and reasonable analytical solution. Li et al. [29] presented the analytic bending solution of a thin plate resting on the Winkler foundation. The governing differential equations of the plate were transferred into Hamilton canonical equations, and the analytic solution could be obtained with all edges slidingly supported. Bai et al. [30] studied the bending problem of the free orthotropic rectangular thin plate (RTP) on a two-parameter elastic foundation under a concentrated load by using the symplectic superposition method. Tenenbaum et al. [31] gave the analytical solutions for the buckling loads of thin rectangular plates with internal supports and different boundary conditions. The solution had a series form, and the coefficients were solved to match the edge conditions. With the development of economy and technology, multilayer structures under static loading or dynamic loading have been delt

with in recent years. Multilayer structures, whose material properties are discontinuous at each interface of the plate, are different from traditional laminated composites. Functionally graded material (FGM) is one of the multilayer structures that is attracting tremendous research interest. The analytical solution for the bending performance of the FGM plate was first introduced in the 1990s [32]. Afterwards, FGM plates were widely used in engineering structures, and the buckling and dynamic response [33–35], post buckling behavior [36,37], and elastoplastic mechanical performances [38–40] of the FGM plates were introduced.

As far as the authors know, there are few studies about the kinematical equations suitable for a stepped rectangular plate. It also seems to be a fact that there are few research papers on the static bending analysis of stepped rectangular plates resting on the elastic half-space foundation. To bridge this gap, this paper used traditional plate theory that is common in the analysis of single plates resting on an elastic foundation. In order to promote the application of traditional plate theories, the stepped rectangular plate is considered to be composed of two plates with different dimensions and properties (upper and lower plates), and taking into account the thickness of the upper and lower plates, the analytical method is divided into three cases: (1) the upper and lower plates are both thin plates; (2) one plate is a thin plate, while the other one is a moderately thick plate; (3) the upper and lower plates are both moderately thick plates. A Fourier series is used to establish the basic equations and the coordination equation of the plate-foundation system, and the boundary conditions are also used to obtain the analytical solution. In addition, the influence of plate theory, the elastic modulus of the plate-foundation system and dimensions of the plate on the bending performance of the stepped rectangular plate are analyzed.

2. Governing Equations and Results

A stepped rectangular plate, whose upper and lower plate dimensions are $a_1 \times b_1$ (length × width) and $a_2 \times b_2$ (length × width), respectively, is referred to the Cartesian systems of coordinates x_1y_1 and x_2y_2 associated with the external surfaces of the upper and lower plates (Figure 1). The contact surface between the upper and lower plates is assumed to exclude their mutual slipping. A uniformly distributed load $q(x_1,y_1)$ is applied on the external surface of upper plate.

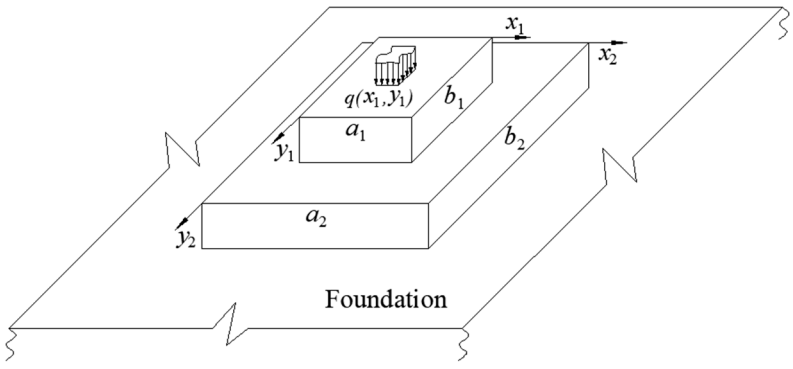

Figure 1. Research model.

2.1. Both Upper and Lower Parts of the Plate Are Thin Plates

2.1.1. Basic Equations and Boundary Conditions

Taking the upper plate as an example, the bending equation of the upper plate can be expressed as [27]:

$$D\nabla^2\nabla^2 w(x,y) = q(x,y) - F(x,y)$$

where $w(x,y)$ is the deflection of the plate, D is the bending stiffness, $q(x,y)$ and $F(x,y)$ are the loadings applied on upper and lower surface of the plate, respectively, and $\nabla^2 = \frac{\partial^2}{\partial y^2} + \frac{\partial^2}{\partial x^2}$ is the Laplacian operator.

Therefore, in the analysis process of the stepped rectangular plate resting on the elastic half-space foundation (Figure 1), the force of the upper and lower plates is different. The

upper and lower loadings applied on the upper plate are $q(x_1,y_1)$ and $F(x_1,y_1)$, respectively, while for the lower plate, these two values are $F(x_1,y_1)$ and $Q(x_2,y_2)$, respectively, in which $F(x_1,y_1)$ and $Q(x_2,y_2)$ are the interaction force between the upper and lower plates and the subgrade reaction, respectively. After that, the bending equation of the upper and lower plates can be written as below:

$$D_{x_1}\frac{\partial^4 w_1}{\partial {x_1}^4} + 2H_1\frac{\partial^4 w_1}{\partial {x_1}^2 \partial {y_1}^2} + D_{y_1}\frac{\partial^4 w_1}{\partial {y_1}^4} + F(x_1,y_1) = q(x_1,y_1) \tag{1a}$$

$$D_{x_2}\frac{\partial^4 w_2}{\partial {x_2}^4} + 2H_2\frac{\partial^4 w_2}{\partial {x_2}^2 \partial {y_2}^2} + D_{y_2}\frac{\partial^4 w_2}{\partial {y_2}^4} + Q(x_2,y_2) = F(x_1,y_1) \tag{1b}$$

where $D_{x_i} = E_{x_i}h_i^3/12(1-v_{x_i}^2)$ and $D_{y_i} = E_{y_i}h_i^3/12(1-v_{y_i}^2)$ are the bending stiffness of x_i-axis direction and y_i-axis direction, respectively. w_i is deflection of the plate, h_i is the thickness of plate, v_{x_i} and v_{y_i} are the Poisson ratio of x_i-axis direction and y_i-axis direction respectively, $H_i = D_{x_i}v_{y_i} + 2D_{x_iy_i}$ is equivalent stiffness, and $D_{x_iy_i}$ is torsional stiffness. The upper and lower plates are numbered i = 1 and i = 2, respectively.

The internal force of the upper and lower plates could be written in terms of deflection functions:

$$M_{x_i} = -D_{x_i}\left(\frac{\partial^2 w_i}{\partial x_i^2} + v_{y_i}\frac{\partial^2 w_i}{\partial y_i^2}\right)$$

$$M_{y_i} = -D_{y_i}\left(\frac{\partial^2 w_i}{\partial y_i^2} + v_{x_i}\frac{\partial^2 w_i}{\partial x_i^2}\right)$$

$$M_{x_iy_i} = -2D_{x_iy_i}\frac{\partial^2 w_i}{\partial x_i \partial y_i}$$

$$Q_{x_i} = -D_{x_i}\frac{\partial^3 w_i}{\partial x_i^3} - (H_i + 2D_{x_iy_i})\frac{\partial^3 w_i}{\partial x_i \partial y_i^2}$$

$$Q_{y_i} = -D_{y_i}\frac{\partial^3 w_i}{\partial y_i^3} - (H_i + 2D_{x_iy_i})\frac{\partial^3 w_i}{\partial y_i \partial x_i^2}$$

$$R_{x_iy_i} = -2D_{x_iy_i}(1-v)\frac{\partial^2 w_i}{\partial x_i \partial y_i}$$

in which M_{x_i} and M_{y_i} are the bending moment of the x_i-axis direction and y_i-axis direction, respectively, $M_{x_iy_i}$ is the twisting moment, Q_{x_i} and Q_{y_i} are the shear force of the x_i-axis direction and y_i-axis direction, respectively, and R is the counterforce at the corner of the upper and lower plates.

The boundary restrictions are given as:

At x = 0, x = a

$$\frac{\partial^2 w_i}{\partial x_i^2} + v_{y_i}\frac{\partial^2 w_i}{\partial y_i^2} = 0\ (M_{x_i} = 0) \tag{2a}$$

$$D_{x_i}\frac{\partial^3 w_i}{\partial x_i^3} + (H_i + 2D_{x_iy_i})\frac{\partial^3 w_i}{\partial x_i \partial y_i^2} = 0\ (Q_{x_i} = 0) \tag{2b}$$

At y = 0, y = a

$$\frac{\partial^2 w_i}{\partial y_i^2} + v_{x_i}\frac{\partial^2 w_i}{\partial x_i^2} = 0\ \left(M_{y_i} = 0\right) \tag{2c}$$

$$D_{y_i}\frac{\partial^3 w_i}{\partial y_i^3} + (H_i + 2D_{x_iy_i})\frac{\partial^3 w_i}{\partial y_i \partial x_i^2} = 0\ (Q_{x_i} = 0) \tag{2d}$$

At the corner of the plate

$$\frac{\partial^2 w_i}{\partial x_i \partial y_i} = 0 \ \left(R_{x_i y_i} = 0\right) \tag{2e}$$

2.1.2. Coordination Equation and Analytical Solution

The deflections of the upper and lower plates can be expressed as a double cosine series with supplementary terms [27] (Appendix A):

$$\begin{aligned} w_i = & \sum_{m_i=0}^{\infty}\sum_{n_i=0}^{\infty} w_{m_i n_i} \cos\frac{m_i \pi x_i}{a_i} \cos\frac{n_i \pi y_i}{b_i} + \sum_{m_i=0}^{\infty}\left\{\left[\mu_{2m_i y_i}\frac{{m_i}^2\pi^2{b_i}^2}{{a_i}^2}\cdot\frac{4b_i{y_i}^3-4{b_i}^2{y_i}^2-{y_i}^4}{24{b_i}^4}\right.\right. \\ & \left.+\frac{2b_i y_i-{y_i}^2}{2{b_i}^2}\right]C_{m_i} + \left[\mu_{2m_i y_i}\frac{{m_i}^2\pi^2{b_i}^2}{{a_i}^2}\cdot\frac{{y_i}^4-2{b_i}^2{y_i}^2}{24{b_i}^4} + \frac{{y_i}^2}{2{b_i}^2}\right]D_{m_i}\Big\}\cos\frac{m_i\pi x_i}{a_i} \\ & + \sum_{n_i=0}^{\infty}\left\{\left[\mu_{2m_i x_i}\frac{{n_i}^2\pi^2{a_i}^2}{{b_i}^2}\cdot\frac{4a_i{x_i}^3-4{a_i}^2{x_i}^2-{x_i}^4}{24{a_i}^4} + \frac{2a_i x_i-{x_i}^2}{2{a_i}^2}\right]G_{n_i} + \left[\mu_{2n_i x_i}\frac{{n_i}^2\pi^2{a_i}^2}{{b_i}^2}\right.\right. \\ & \left.\cdot\frac{{x_i}^4-2{a_i}^2{x_i}^2}{24{a_i}^4} + \frac{{x_i}^2}{2{a_i}^2}\right]H_{n_i}\Big\}\cos\frac{n_i\pi y_i}{b_i} \\ & (m_i = 0,1,2,\cdots;\quad n_i = 0,1,2,\cdots) \end{aligned} \tag{3}$$

where $\mu_{2n_i x_i} = \frac{H_i+2D_{x_i y_i}}{D_{x_i}}$, $\mu_{2m_i y_i} = \frac{H_i+2D_{x_i y_i}}{D_{y_i}}$, $w_{m_i n_i}$, C_{m_i}, D_{m_i}, G_{n_i}, H_{n_i} are undetermined parameters.

Equation (4) has four steps' derivation for a rectangular plate with four free edges, which could satisfy the boundary conditions, such as the shear force at the boundary (Equation (2b,d)) and the corner condition (Equation (2e)). If the plate is made of isotropic material, the Equation (4) can degenerate into an expression of an isotropic rectangular plate.

Based on Equation (1a,b), it could be found that $F(x_1,y_1)$ is related to the control differential equations of the upper and lower plates, so $F(x_1,y_1)$ can be expanded into a double cosine series represented by x_1, y_1 and x_2, y_2.

$$F(x_1,y_1) = \sum_{m_1=0}^{\infty}\sum_{n_1=0}^{\infty}\lambda_{m_1 n_1}F_{m_1 n_1}\cos\frac{m_1\pi x_1}{a_1}\cos\frac{n_1\pi y_1}{b_1} \tag{4}$$

$$\begin{gathered} F(x_2,y_2) = \sum_{m_2=0}^{\infty}\sum_{n_2=0}^{\infty}\lambda_{m_2 n_2}F_{m_2 n_2}\cos\frac{m_2\pi x_2}{a_2}\cos\frac{n_2\pi y_2}{b_2} \\ (m_i = 0,1,2,\cdots;\quad n_i = 0,1,2,\cdots) \end{gathered} \tag{5}$$

where

$$\lambda_{m_i n_i} = \begin{cases} 1/4,\ m_i = n_i = 0 \\ 1/2,\ m_i = 0,\ n_i > 0\ or\ m_i > 0,\ n_i = 0 \\ 1/4,\ m_i > 0,\ n_i > 0 \end{cases}$$

$$F_{m_1 n_1} = \frac{4}{a_1 b_1}\int_0^{b_1}\int_0^{a_1} F_1(x_1,y_1)\cos\frac{m_1\pi x_1}{a_1}\cos\frac{n_1\pi y_1}{b_1}dx_1 dy_1$$

$$\begin{aligned} & F_{m_2 n_2} = \tfrac{4}{a_2 b_2}\textstyle\int_0^{b_2}\int_0^{a_2} F(x_1,y_1)\cos\frac{m_2\pi x_2}{a_2}\cos\frac{n_2\pi y_2}{b_2}dx_2 dy_2 \\ & = \tfrac{4}{a_2 b_2}\textstyle\int_0^{b_2}\int_0^{a_2}\sum_{m_1=0}^{\infty}\sum_{n_1=0}^{\infty}\lambda_{m_1 n_1}F_{m_1 n_1}\cos\frac{m_1\pi x_1}{a_1}\cos\frac{n_1\pi y_1}{b_1}\cos\frac{m_2\pi x_2}{a_2}\cos\frac{n_2\pi y_2}{b_2}dx_2 dy_2 \\ & = \tfrac{4}{a_2 b_2}\textstyle\sum_{m_1=0}^{\infty}\sum_{n_1=0}^{\infty}\int_0^{b_2}\int_0^{a_2}\lambda_{m_1 n_1}F_{m_1 n_1}\cos\frac{m_1\pi x_1}{a_1}\cos\frac{n_1\pi y_1}{b_1}\cos\frac{m_2\pi x_2}{a_2}\cos\frac{n_2\pi y_2}{b_2}dx_2 dy_2 \\ & = \tfrac{4}{a_2 b_2}\textstyle\sum_{m_1=0}^{\infty}\sum_{n_1=0}^{\infty}\lambda_{m_1 n_1}F_{m_1 n_1}\int_0^{b_2}\int_0^{a_2}\cos\frac{m_1\pi x_1}{a_1}\cos\frac{n_1\pi y_1}{b_1}\cos\frac{m_2\pi x_2}{a_2}\cos\frac{n_2\pi y_2}{b_2}dx_2 dy_2 \\ & (m_i = 0,1,2,\cdots;\quad n_i = 0,1,2,\cdots) \end{aligned}$$

x_0, y_0 represent the relationship between the x_1y_1 and x_2y_2 coordinate systems, and substituting $x_2 = x_1 + x_0$, $y_2 = y_1 + y_0$ into the integral part of expression of $F_{m_2n_2}$:

$$\begin{aligned}
&\int_0^{b_2}\int_0^{a_2}\cos\tfrac{m_1\pi x_1}{a_1}\cos\tfrac{n_1\pi y_1}{b_1}\cos\tfrac{m_2\pi x_2}{a_2}\cos\tfrac{n_2\pi y_2}{b_2}dx_2dy_2\\
&=\int_{x_0}^{x_0+a_1}\int_{y_0}^{y_0+b_1}\cos\tfrac{m_1\pi x_1}{a_1}\cos\tfrac{n_1\pi y_1}{b_1}\cos\tfrac{m_2\pi x_2}{a_2}\cos\tfrac{n_2\pi y_2}{b_2}dx_2dy_2\\
&=\int_{x_0}^{x_0+a_1}\int_{y_0}^{y_0+b_1}\cos\tfrac{m_1\pi(x_2-x_0)}{a_1}\cos\tfrac{n_1\pi(y_2-y_0)}{b_1}\cos\tfrac{m_2\pi x_2}{a_2}\cos\tfrac{n_2\pi y_2}{b_2}dx_2dy_2\\
&=\left\{\tfrac{1}{2}\cos\tfrac{m_1\pi x_0}{a_1}\tfrac{a_2a_1}{\pi(m_1a_2+m_2a_1)}\left[\sin\tfrac{\pi(m_1a_2+m_2a_1)(x_0+a_1)}{a_2a_1}-\sin\tfrac{\pi(m_1a_2+m_1a_1)x_0}{a_2a_1}\right]\right.\\
&+\tfrac{1}{2}\cos\tfrac{m_1\pi x_0}{a_1}\tfrac{a_2a_1}{\pi(m_1a_2-m_2a_1)}\left[\sin\tfrac{\pi(m_1a_2-m_2a_1)(x_0+a_1)}{a_2a_1}-\sin\tfrac{\pi(m_1a_2-m_2a_1)x_0}{a_2a_1}\right]\\
&+\tfrac{1}{2}\sin\tfrac{m_1\pi x_0}{a_1}\tfrac{a_2a_1}{\pi(m_1a_2+m_2a_1)}\left[\cos\tfrac{\pi(m_1a_2+m_2a_1)x_0}{a_2a_1}-\cos\tfrac{\pi(m_1a_2+m_2a_1)(x_0+a_1)}{a_2a_1}\right]\\
&\left.+\tfrac{1}{2}\sin\tfrac{m_1\pi x_0}{a_1}\tfrac{a_2a_1}{\pi(m_1a_2-m_2a_1)}\left[\cos\tfrac{\pi(m_1a_2-m_2a_1)x_0}{a_2a_1}-\cos\tfrac{\pi(m_1a_2-m_2a_1)(x_0+a_1)}{a_2a_1}\right]\right\}\\
&\cdot\left\{\tfrac{1}{2}\cos\tfrac{n_1\pi y_0}{b_1}\tfrac{b_2b_1}{\pi(n_1b_2+n_2b_1)}\left[\sin\tfrac{\pi(n_1b_2+n_2b_1)(y_0+b_1)}{b_2b_1}-\sin\tfrac{\pi(n_1b_2+n_1b_1)y_0}{b_2b_1}\right]\right.\\
&+\tfrac{1}{2}\cos\tfrac{n_1\pi y_0}{b_1}\tfrac{b_2b_1}{\pi(n_1b_2-n_2b_1)}\left[\sin\tfrac{\pi(n_1b_2-n_2b_1)(y_0+b_1)}{b_2b_1}-\sin\tfrac{\pi(n_1b_2-n_2b_1)y_0}{b_2b_1}\right]\\
&+\tfrac{1}{2}\sin\tfrac{n_1\pi y_0}{b_1}\tfrac{b_2b_1}{\pi(n_1b_2+n_2b_1)}\left[\cos\tfrac{\pi(n_1b_2+n_2b_1)y_0}{b_2b_1}-\cos\tfrac{\pi(n_1b_2+n_2b_1)(y_0+b_1)}{b_2b_1}\right]\\
&\left.+\tfrac{1}{2}\sin\tfrac{n_1\pi y_0}{b_1}\tfrac{b_2b_1}{\pi(n_1b_2-n_2b_1)}\left[\cos\tfrac{\pi(n_1b_2-n_2b_1)y_0}{b_2b_1}-\cos\tfrac{\pi(n_1b_2-n_2b_1)(y_0+b_1)}{b_2b_1}\right]\right\}\\
&=B\\
&(m_i=0,1,2,\cdots;\quad n_i=0,1,2,\cdots)
\end{aligned}$$

Hence, the expression for $F_{m_2n_2}$ is rewritten as

$$F_{m_2n_2}=\frac{4}{a_2b_2}\sum_{m_1=0}^{\infty}\sum_{n_1=0}^{\infty}\lambda_{m_1n_1}F_{m_1n_1}B$$

$q(x_1,y_1)$ is expanded into a double cosine series represented by x_1 and y_1.

$$\begin{gathered}q(x_1,y_1)=\sum_{m_1=0}^{\infty}\sum_{n_1=0}^{\infty}\lambda_{m_1n_1}q_{m_1n_1}\cos\frac{m_1\pi x_1}{a_1}\cos\frac{n_1\pi y_1}{b_1}\\(m_i=0,1,2,\cdots;\quad n_i=0,1,2,\cdots)\end{gathered}\tag{6}$$

where

$$q_{m_1n_1}=\frac{4}{a_1b_1}\int_0^{b_1}\int_0^{a_1}q(x_1,y_1)\cos\frac{m_1\pi x_1}{a_1}\cos\frac{n_1\pi y_1}{b_1}dx_1dy_1$$

The subgrade reaction can be expressed in terms of the double cosine series as

$$Q(x_2,y_2)=\sum_{m_2=0}^{\infty}\sum_{n_2=0}^{\infty}\lambda_{m_2n_2}Q_{m_2n_2}\cos\frac{m_2\pi x_2}{a_2}\cos\frac{n_2\pi y_2}{b_2}$$

where

$$Q_{m_2n_2}=\frac{4}{a_2b_2}\int_0^{b_2}\int_0^{a_2}Q(x_2,y_2)\cos\frac{m_2\pi x_2}{a_2}\cos\frac{n_2\pi y_2}{b_2}dx_2dy_2$$

Substituting Equations (3)–(6) into Equation (1a,b), and then expanding the polynomial of the supplementary terms in the formulas to the cosine series. Comparing the coefficients

of the corresponding items on both sides of the Equation (1a,b), the expressions can be obtained as:

$$
\begin{aligned}
&[D_{x_1}\alpha_{m_1}{}^4 + 2H_1\alpha^4{}_{m_1}{}^2\beta_{n_1}{}^2 + D_{y_1}\beta_{n_1}{}^4]w_{m_1n_1} + \\
&\left\{2D_{x_1}\alpha_{m_1}{}^4\left[\tfrac{H_1+2D_{x_1y_1}}{D_{y_1}}\cdot\tfrac{m_1{}^2\pi^2b_1{}^2}{a_1{}^2}\left(\tfrac{h_{n_1}}{\beta_{n_1}{}^4b_1{}^4}-\tfrac{\overline{h_{n_1}}}{90}\right)-\tfrac{h_{n_1}}{\beta_{n_1}{}^2b_1{}^2}+\tfrac{\overline{h_{n_1}}}{6}\right]+\right. \\
&\left.2H_1\alpha_{m_1}{}^4\cdot\tfrac{2(H_1+2D_{x_1y_1})}{D_{y_1}\beta_{n_1}{}^2b_1{}^2}h_{n_1}+\tfrac{\alpha_{m_1}{}^2}{b_1{}^2}\left[H_1-2D_{x_1y_1}\right]\overline{h_{n_1}}\right\}C_{m_1} + \\
&\left\{2D_{x_1}\alpha_{m_1}{}^4\left[\tfrac{H_1+2D_{x_1y_1}}{D_{y_1}}\cdot\tfrac{m_1{}^2\pi^2b_1{}^2}{a_1{}^2}\left(\tfrac{h_{n_1}}{\beta_{n_1}{}^4b_1{}^4}+\tfrac{7\overline{h_{n_1}}}{720}\right)-\tfrac{h_{n_1}}{\beta_{n_1}{}^2b_1{}^2}-\tfrac{\overline{h_{n_1}}}{12}\right]+\right. \\
&\left.2H_1\alpha_{m_1}{}^4\cdot\tfrac{2(H_1+2D_{x_1y_1})}{D_{y_1}\beta_{n_1}{}^2b_1{}^2}h_{n_1}+\tfrac{\alpha_{m_1}{}^2}{b_1{}^2}\left[H_1-2D_{x_1y_1}\right]\overline{h_{n_1}}\right\}(-1)^{n_1+1}D_{m_1} + \\
&\left\{2D_{y_1}\beta_{n_1}{}^4\left[\tfrac{H_1+2D_{x_1y_1}}{D_{x_1}}\cdot\tfrac{n_1{}^2\pi^2a_1{}^2}{b_1{}^2}\left(\tfrac{h_{m_1}}{\alpha_{m_1}{}^4a_1{}^4}-\tfrac{\overline{h_{m_1}}}{90}\right)-\tfrac{h_{m_1}}{\alpha_{m_1}{}^2a_1{}^2}+\tfrac{\overline{h_{m_1}}}{6}\right]+\right. \\
&\left.2H_1\beta_{n_1}{}^4\cdot\tfrac{2(H_1+2D_{x_1y_1})}{D_{x_1}\alpha_{m_1}{}^2a_1{}^2}h_{m_1}+\tfrac{\beta_{n_1}{}^2}{a_1{}^2}\left[H_1-2D_{x_1y_1}\right]\overline{h_{m_1}}\right\}G_{n_1} + \\
&\left\{2D_{y_1}\beta_{n_1}{}^4\left[\tfrac{H_1+2D_{x_1y_1}}{D_{x_1}}\cdot\tfrac{n_1{}^2\pi^2a_1{}^2}{b_1{}^2}\left(\tfrac{h_{m_1}}{\alpha_{m_1}{}^4a_1{}^4}+\tfrac{7\overline{h_{m_1}}}{720}\right)-\tfrac{h_{m_1}}{\alpha_{m_1}{}^2a_1{}^2}-\tfrac{\overline{h_{m_1}}}{12}\right]+\right. \\
&\left.2H_1\beta_{n_1}{}^4\cdot\tfrac{2(H_1+2D_{x_1y_1})}{D_{x_1}\alpha_{m_1}{}^2a_1{}^2}h_{m_1}+\tfrac{\beta_{n_1}{}^2}{a_1{}^2}\left[H_1-2D_{x_1y_1}\right]\overline{h_{m_1}}\right\}(-1)^{m_1+1}H_{n_1} \\
&=\lambda_{m_1n_1}(q_{m_1n_1}-F_{m_1n_1}) \\
&(m_1=0,1,2,\cdots;\quad n_1=0,1,2,\cdots)
\end{aligned}
\tag{7}
$$

$$
\begin{aligned}
&[D_{x_2}\alpha_{m_2}{}^4 + 2H_2\alpha^4{}_{m_2}{}^2\beta_{n_2}{}^2 + D_{y_2}\beta_{n_2}{}^4]w_{m_2n_2} + \\
&\left\{2D_{x_2}\alpha_{m_2}{}^4\left[\tfrac{H_2+2D_{x_2y_2}}{D_{y_2}}\cdot\tfrac{m_2{}^2\pi^2b_2{}^2}{a_2{}^2}\left(\tfrac{h_{n_2}}{\beta_{n_2}{}^4b_2{}^4}-\tfrac{\overline{h_{n_2}}}{90}\right)-\tfrac{h_{n_2}}{\beta_{n_2}{}^2b_2{}^2}+\tfrac{\overline{h_{n_2}}}{6}\right]+\right. \\
&\left.2H_2\alpha_{m_2}{}^4\cdot\tfrac{2(H_2+2D_{x_2y_2})}{D_{y_2}\beta_{n_2}{}^2b_2{}^2}h_{n_2}+\tfrac{\alpha_{m_2}{}^2}{b_2{}^2}\left[H_2-2D_{x_2y_2}\right]\overline{h_{n_2}}\right\}C_{m_2} + \\
&\left\{2D_{x_2}\alpha_{m_2}{}^4\left[\tfrac{H_2+2D_{x_2y_2}}{D_{y_2}}\cdot\tfrac{m_2{}^2\pi^2b_2{}^2}{a_2{}^2}\left(\tfrac{h_{n_2}}{\beta_{n_2}{}^4b_2{}^4}+\tfrac{7\overline{h_{n_2}}}{720}\right)-\tfrac{h_{n_2}}{\beta_{n_2}{}^2b_2{}^2}-\tfrac{\overline{h_{n_2}}}{12}\right]+\right. \\
&\left.2H_2\alpha_{m_2}{}^4\cdot\tfrac{2(H_2+2D_{x_2y_2})}{D_{y_2}\beta_{n_2}{}^2b_2{}^2}h_{n_2}+\tfrac{\alpha_{m_2}{}^2}{b_2{}^2}\left[H_2-2D_{x_2y_2}\right]\overline{h_{n_2}}\right\}(-1)^{n_2+1}D_{m_2} + \\
&\left\{2D_{y_2}\beta_{n_2}{}^4\left[\tfrac{H_2+2D_{x_2y_2}}{D_{x_2}}\cdot\tfrac{n_2{}^2\pi^2a_2{}^2}{b_2{}^2}\left(\tfrac{h_{m_2}}{\alpha_{m_2}{}^4a_2{}^4}-\tfrac{\overline{h_{m_2}}}{90}\right)-\tfrac{h_{m_2}}{\alpha_{m_2}{}^2a_2{}^2}+\tfrac{\overline{h_{m_2}}}{6}\right]+\right. \\
&\left.2H_2\beta_{n_2}{}^4\cdot\tfrac{2(H_2+2D_{x_2y_2})}{D_{x_2}\alpha_{m_2}{}^2a_2{}^2}h_{m_2}+\tfrac{\beta_{n_2}{}^2}{a_2{}^2}\left[H_2-2D_{x_2y_2}\right]\overline{h_{m_2}}\right\}G_{n_2} + \\
&\left\{2D_{y_2}\beta_{n_2}{}^4\left[\tfrac{H_2+2D_{x_2y_2}}{D_{x_2}}\cdot\tfrac{n_2{}^2\pi^2a_2{}^2}{b_2{}^2}\left(\tfrac{h_{m_2}}{\alpha_{m_2}{}^4a_2{}^4}+\tfrac{7\overline{h_{m_2}}}{720}\right)-\tfrac{h_{m_2}}{\alpha_{m_2}{}^2a_2{}^2}-\tfrac{\overline{h_{m_2}}}{12}\right]+\right. \\
&\left.2H_2\beta_{n_2}{}^4\cdot\tfrac{2(H_2+2D_{x_2y_2})}{D_{x_2}\alpha_{m_2}{}^2a_2{}^2}h_{m_2}+\tfrac{\beta_{n_2}{}^2}{a_2{}^2}\left[H_2-2D_{x_2y_2}\right]\overline{h_{m_2}}\right\}(-1)^{m_2+1}H_{n_2} \\
&=\lambda_{m_2n_2}(F_{m_2n_2}-Q_{m_2n_2}) \\
&(m_2=0,1,2,\cdots;\quad n_2=0,1,2,\cdots)
\end{aligned}
\tag{8}
$$

where $\alpha_{m_i}=\frac{m_i\pi}{a_i}$, $\beta_{m_i}=\frac{n_i\pi}{b_i}$, $h_{m_i}=h_{n_i}=\begin{cases}0, i=0\\ 1, i\neq 0\end{cases}$, and $\overline{h_{m_i}}=\overline{h_{n_i}}=\begin{cases}1, i=0\\ 0, i\neq 0\end{cases}$.

Considering the boundary conditions of the bending moment, we could obtain:

(1) When $x_i = 0$, $M_{x_i} = 0$ (Equation (2a)):

$$\begin{array}{l}\sum\limits_{m_i=0}^{\infty}(\alpha_{m_i}^2+v_{y_i}\beta_{n_i}^2)w_{m_in_i}+2\sum\limits_{m_i=0}^{\infty}\left\{\frac{H_i+2D_{x_iy_i}}{D_{y_i}}{b_i}^2\alpha_{m_i}^4\left(\frac{h_{n_i}}{\beta_{n_i}^4{b_i}^4}-\frac{\overline{h}_{n_i}}{90}\right)\right.\\ \left.+\alpha_{m_i}^2\left[-\frac{1}{\beta_{n_i}^2{b_i}^2}h_{n_i}+\frac{\overline{h}_{n_i}}{6}\right]+\alpha_{m_i}^2v_{y_i}\cdot\frac{H_i+2D_{x_iy_i}}{D_{y_i}}\cdot\frac{1}{\beta_{n_i}^2{b_i}^2}h_{n_i}+\frac{v_{y_i}\overline{h}_{n_i}}{2{b_i}^2}\right\}C_{m_i}\\ +2(-1)^{n_i+1}\sum\limits_{m_i=0}^{\infty}\left\{\frac{H_i+2D_{x_iy_i}}{D_{y_i}}{b_i}^2\alpha_{m_i}^4\left(\frac{h_{n_i}}{\beta_{n_i}^4{b_i}^4}+\frac{7\overline{h}_{n_i}}{720}\right)\right.\\ \left.-\alpha_{m_i}^2\left[\frac{1}{\beta_{n_i}^2{b_i}^2}h_{n_i}+\frac{\overline{h}_{n_i}}{12}\right]+\alpha_{m_i}^2v_{y_i}\cdot\frac{H_i+2D_{x_iy_i}}{D_{y_i}}\cdot\frac{1}{\beta_{n_i}^2{b_i}^2}h_{n_i}+\frac{v_{y_i}\overline{h}_{n_i}}{2{b_i}^2}\right\}D_{m_i}\\ +\left(\frac{H_i+2D_{x_iy_i}}{3D_{x_i}}\beta_{n_i}^2+\frac{1}{{a_i}^2}\right)G_{n_i}+\left(\frac{H_i+2D_{x_iy_i}}{6D_{x_i}}\beta_{n_i}^2-\frac{1}{{a_i}^2}\right)H_{n_i}=0\\ (n_i=0,1,2,\cdots)\end{array}\tag{9}$$

(2) When $x_i = a_i$, $M_{x_i} = 0$ (Equation (2a)):

$$\begin{array}{l}\sum\limits_{m_i=0}^{\infty}(-1)^{m_i}(\alpha_{m_i}^2+v_{y_i}\beta_{n_i}^2)w_{m_in_i}+2\sum\limits_{m_i=0}^{\infty}\left\{(-1)^{m_i}\frac{H_i+2D_{x_iy_i}}{D_{y_i}}{b_i}^2\alpha_{m_i}^4\left(\frac{h_{n_i}}{\beta_{n_i}^4{b_i}^4}-\frac{\overline{h}_{n_i}}{90}\right)\right.\\ \left.+\alpha_{m_i}^2\left[-\frac{1}{\beta_{n_i}^2{b_i}^2}h_{n_i}+\frac{\overline{h}_{n_i}}{6}\right]+\alpha_{m_i}^2v_{y_i}\cdot\frac{H_i+2D_{x_iy_i}}{D_{y_i}}\cdot\frac{1}{\beta_{n_i}^2{b_i}^2}h_{n_i}+\frac{v_{y_i}\overline{h}_{n_i}}{2{b_i}^2}\right\}C_{m_i}\\ +2(-1)^{n_i+1}\sum\limits_{m_i=0}^{\infty}\left\{(-1)^{m_i}\frac{H_i+2D_{x_iy_i}}{D_{y_i}}{b_i}^2\alpha_{m_i}^4\left(\frac{h_{n_i}}{\beta_{n_i}^4{b_i}^4}+\frac{7\overline{h}_{n_i}}{720}\right)\right.\\ \left.-\alpha_{m_i}^2\left[\frac{1}{\beta_{n_i}^2{b_i}^2}h_{n_i}+\frac{\overline{h}_{n_i}}{12}\right]+\alpha_{m_i}^2v_{y_i}\cdot\frac{H_i+2D_{x_iy_i}}{D_{y_i}}\cdot\frac{1}{\beta_{n_i}^2{b_i}^2}h_{n_i}+\frac{v_{y_i}\overline{h}_{n_i}}{2{b_i}^2}\right\}D_{m_i}\\ +\left(-\frac{v_{y_i}(H_i+2D_{x_iy_i})}{24D_{x_i}}{a_i}^2\beta_{n_i}^4+\left(\frac{v_{y_i}}{2}-\frac{H_i+2D_{x_iy_i}}{6D_{x_i}}\right)\beta_{n_i}^2+\frac{1}{{a_i}^2}\right)G_{n_i}+\\ \left(-\frac{v_{y_i}(H_i+2D_{x_iy_i})}{24D_{x_i}}{a_i}^2\beta_{n_i}^4+\left(\frac{v_{y_i}}{2}-\frac{H_i+2D_{x_iy_i}}{3D_{x_i}}\right)\beta_{n_i}^2-\frac{1}{{a_i}^2}\right)H_{n_i}=0\\ (n_i=0,1,2,\cdots)\end{array}\tag{10}$$

(3) When $y_i = 0$, $M_{y_i} = 0$ (Equation (2c)):

$$\begin{array}{l}\sum\limits_{n_i=0}^{\infty}(\beta_{n_i}^2+v_{x_i}\alpha_{m_i}^2)w_{m_in_i}+\left(\frac{H_i+2D_{x_iy_i}}{3D_{y_i}}\alpha_{m_i}^2+\frac{1}{{b_i}^2}\right)C_{m_i}+\left(\frac{H_i+2D_{x_iy_i}}{6D_{y_i}}\alpha_{m_i}^2-\frac{1}{{b_i}^2}\right)D_{m_i}\\ +2\sum\limits_{n_i=0}^{\infty}\left\{\frac{H_i+2D_{x_iy_i}}{D_{x_i}}{a_i}^2\beta_{n_i}^4\left(\frac{h_{m_i}}{\alpha_{m_i}^4{a_i}^4}-\frac{\overline{h}_{m_i}}{90}\right)+\beta_{n_i}^2\left[-\frac{1}{\alpha_{m_i}^2{a_i}^2}h_{m_i}+\frac{\overline{h}_{m_i}}{6}\right]\right.\\ \left.+\beta_{n_i}^2v_{x_i}\cdot\frac{H_i+2D_{x_iy_i}}{D_{x_i}}\cdot\frac{1}{\alpha_{m_i}^2{a_i}^2}h_{m_i}+\frac{v_{x_i}\overline{h}_{m_i}}{2{a_i}^2}\right\}G_{n_i}\\ +2(-1)^{m_i+1}\sum\limits_{n_i=0}^{\infty}\left\{\frac{H_i+2D_{x_iy_i}}{D_{x_i}}{a_i}^2\beta_{n_i}^4\left(\frac{h_{m_i}}{\alpha_{m_i}^4{a_i}^4}+\frac{7\overline{h}_{m_i}}{720}\right)\right.\\ \left.-\beta_{n_i}^2\left[\frac{1}{\alpha_{m_i}^2{a_i}^2}h_{m_i}+\frac{\overline{h}_{m_i}}{12}\right]+\beta_{n_i}^2v_{x_i}\cdot\frac{H_i+2D_{x_iy_i}}{D_{x_i}}\cdot\frac{1}{\alpha_{m_i}^2{a_i}^2}h_{m_i}+\frac{v_{x_i}\overline{h}_{m_i}}{2{a_i}^2}\right\}H_{n_i}=0\\ (m_i=0,1,2,\cdots)\end{array}\tag{11}$$

(4) When $y_i = b_i$, $M_{y_i} = 0$ (Equation (2c)):

$$\begin{array}{l}+2\sum\limits_{n_i=0}^{\infty}\left\{(-1)^{n_i}\frac{H+2D_{x_iy_i}}{D_{x_i}}{a_i}^2\beta_{n_i}^4\left(\frac{h_{m_i}}{\alpha_{m_i}^4{a_i}^4}-\frac{\overline{h}_{m_i}}{90}\right)+\beta_{n_i}^2\left[-\frac{1}{\alpha_{m_i}^2{a_i}^2}h_{m_i}+\frac{\overline{h}_{m_i}}{6}\right]\right.\\ \left.+\beta_{n_i}^2v_{x_i}\cdot\frac{H_i+2D_{x_iy_i}}{D_{x_i}}\cdot\frac{1}{\alpha_{m_i}^2{a_i}^2}h_{m_i}+\frac{v_{x_i}\overline{h}_{m_i}}{2{a_i}^2}\right\}G_{n_i}\\ +2(-1)^{m_i+1}\sum\limits_{n_i=0}^{\infty}\left\{(-1)^{n_i}\frac{H_i+2D_{x_iy_i}}{D_{x_i}}{a_i}^2\beta_{n_i}^4\left(\frac{h_{m_i}}{\alpha_{m_i}^4{a_i}^4}+\frac{7\overline{h}_{m_i}}{720}\right)\right.\\ \left.-\beta_{n_i}^2\left[\frac{1}{\alpha_{m_i}^2{a_i}^2}h_{m_i}+\frac{\overline{h}_{m_i}}{12}\right]+\beta_{n_i}^2v_{x_i}\cdot\frac{H_i+2D_{x_iy_i}}{D_{x_i}}\cdot\frac{1}{\alpha_{m_i}^2{a_i}^2}h_{m_i}+\frac{v_{x_i}\overline{h}_{m_i}}{2{a_i}^2}\right\}H_{n_i}=0\\ (m_i=0,1,2,\cdots)\end{array}\tag{12}$$

The deflection of the upper and lower plates could be expressed by formula [27]:

$$w_i(x_i,y_i)=\sum_{m_i=0}^{\infty}\sum_{n_i=0}^{\infty}\lambda_{m_in_i}w_{im_in_i}\cos\frac{m_i\pi x_i}{a_i}\cos\frac{n_i\pi y_i}{b_i}$$

where

$$w_{im_in_i} = \frac{4}{a_ib_i}\int_0^{b_i}\int_0^{a_i} w_i(x_i,y_i)\cos\frac{m_i\pi x_i}{a_i}\cos\frac{n_i\pi y_i}{b_i}dx_idy_i$$

$$\begin{aligned}
&w_{im_in_i} = w_{m_in_i} + 2\left[\mu_{2m_iy_i}{b_i}^2\alpha_{m_i}^2\left(\frac{h_{n_i}}{\beta_{n_i}^4{b_i}^4} - \frac{\overline{h}_{n_i}}{90}\right) - \frac{h_{n_i}}{\beta_{n_i}^2{b_i}^2} + \frac{\overline{h}_{n_i}}{6}\right]C_{m_i}\\
&+2\left[\mu_{2m_iy_i}{b_i}^2\alpha_{m_i}^2\left(\frac{h_{n_i}}{\beta_{n_i}^4{b_i}^4} + \frac{7\overline{h}_{n_i}}{720}\right) - \frac{h_{n_i}}{\beta_{n_i}^2{b_i}^2} - \frac{\overline{h}_{n_i}}{12}\right](-1)^{n_i+1}D_{m_i}\\
&+2\left[\mu_{2m_ix_i}{a_i}^2\beta_{n_i}^2\left(\frac{h_{m_i}}{\alpha_{m_i}^4{a_i}^4} - \frac{\overline{h}_{m_i}}{90}\right) - \frac{h_{m_i}}{\alpha_{m_i}^2{a_i}^2} + \frac{\overline{h}_{m_i}}{6}\right]G_{n_i}\\
&+2\left[\mu_{2m_ix_i}{a_i}^2\beta_{n_i}^2\left(\frac{h_{m_i}}{\alpha_{m_i}^4{a_i}^4} + \frac{7\overline{h}_{m_i}}{720}\right) - \frac{h_{m_i}}{\alpha_{m_i}^2{a_i}^2} - \frac{\overline{h}_{m_i}}{12}\right](-1)^{m_i+1}H_{n_i}\\
&(m_i = 0,1,2,\cdots;\quad n_i = 0,1,2,\cdots)
\end{aligned}$$

Expanding the deflections of the lower plate into the double cosine series at the contacting position with the upper plate:

$$w_2(x_1,y_1) = \sum_{m_1=0}^{\infty}\sum_{n_1=0}^{\infty}\lambda_{m_1n_1}W_{2m_1n_1}\cos\frac{m_1\pi x_1}{a_1}\cos\frac{n_1\pi y_1}{b_1}$$

$$\begin{aligned}
&w_{2m_1n_1} = \tfrac{4}{a_1b_1}\textstyle\int_0^{b_1}\int_0^{a_1} W_2(x_2,y_2)\cos\frac{m_1\pi x_1}{a_1}\cos\frac{n_1\pi y_1}{b_1}dx_1dy_1\\
&= \tfrac{4}{a_1b_1}\textstyle\int_0^{b_1}\int_0^{a_1}\sum_{m_2=0}^{\infty}\sum_{n_2=0}^{\infty}\lambda_{m_2n_2}W_{2m_2n_2}\cos\frac{m_2\pi x_2}{a_2}\cos\frac{n_2\pi y_2}{b_2}\cos\frac{m_1\pi x_1}{a_1}\cos\frac{n_1\pi y_1}{b_1}dx_1dy_1\\
&= \tfrac{4}{a_1b_1}\textstyle\sum_{m_2=0}^{\infty}\sum_{n_2=0}^{\infty}\lambda_{m_2n_2}W_{2m_2n_2}\int_0^{b_1}\int_0^{a_1}\cos\frac{m_2\pi x_2}{a_2}\cos\frac{n_2\pi y_2}{b_2}\cos\frac{m_1\pi x_1}{a_1}\cos\frac{n_1\pi y_1}{b_1}dx_1dy_1\\
&(m_i = 0,1,2,\cdots;\quad n_i = 0,1,2,\cdots)
\end{aligned}$$

Substituting $x_2 = x_1 + x_0$ and $y_2 = y_1 + y_0$ into the expression of $w_{2m_1n_1}$, we obtain:

$$\begin{aligned}
&\textstyle\int_0^{b_1}\int_0^{a_1}\cos\frac{m_2\pi x_2}{a_2}\cos\frac{n_2\pi y_2}{b_2}\cos\frac{m_1\pi x_1}{a_1}\cos\frac{n_1\pi y_1}{b_1}dx_1dy_1\\
&= \textstyle\int_0^{b_1}\int_0^{a_1}\cos\frac{m_2\pi(x_1+x_0)}{a_2}\cos\frac{n_2\pi(y_1+y_0)}{b_2}\cos\frac{m_1\pi x_1}{a_1}\cos\frac{n_1\pi y_1}{b_1}dx_1dy_1\\
&= \left\{\tfrac{1}{2}\cos\frac{m_2\pi x_0}{a_2}\frac{a_2a_1}{\pi(m_2a_1+m_1a_2)}\sin\frac{\pi a_1(m_2a_1+m_1a_2)}{a_2a_1}\right.\\
&+\tfrac{1}{2}\cos\frac{m_2\pi x_0}{a_2}\frac{a_2a_1}{\pi(m_2a_1-m_1a_2)}\sin\frac{\pi c(m_2a_1-m_1a_2)}{a_2a_1}\\
&-\tfrac{1}{2}\sin\frac{m_2\pi x_0}{a_2}\frac{a_2a_1}{\pi(m_2a_1+m_1a_2)}\left[1-\cos\frac{\pi c(m_2a_1+m_1a_2)}{a_2a_1}\right]\\
&\left.-\tfrac{1}{2}\sin\frac{m_2\pi x_0}{a_2}\frac{a_2a_1}{\pi(m_2a_1-m_1a_2)}\left[1-\cos\frac{\pi a_1(m_2a_1-m_1a_2)}{a_2a_1}\right]\right\}\\
&\cdot\left\{\tfrac{1}{2}\cos\frac{n_2\pi y_0}{b_2}\frac{b_2b_1}{\pi(n_2b_1+n_1b_2)}\sin\frac{\pi b_1(n_2b_1+n_1b_2)}{b_2b_1}\right.\\
&+\tfrac{1}{2}\cos\frac{n_2\pi y_0}{b_2}\frac{b_2b_1}{\pi(n_2b_1-n_1b_2)}\sin\frac{\pi b_1(n_2b_1-n_1b_2)}{b_2b_1}\\
&-\tfrac{1}{2}\sin\frac{n_2\pi y_0}{b_2}\frac{b_2b_1}{\pi(n_2b_1+n_1b_2)}\left[1-\cos\frac{\pi d(n_2b_1+n_1b_2)}{b_2b_1}\right]\\
&\left.-\tfrac{1}{2}\sin\frac{n_2\pi y_0}{b_2}\frac{b_2b_2}{\pi(n_2b_1-n_1b_2)}\left[1-\cos\frac{\pi b_1(n_2b_1-n_1b_2)}{b_2b_1}\right]\right\} = D\\
&(m_i = 0,1,2,\cdots;\quad n_i = 0,1,2,\cdots)
\end{aligned}$$

The expression of $w_{2m_1n_1}$ can be rewritten as:

$$W_{2m_1n_1} = \frac{4}{a_1b_1}\sum_{m_2=0}^{\infty}\sum_{n_2=0}^{\infty}\lambda_{m_2n_2}W_{2m_2n_2}D$$

Taking into account that the deflections of the upper and lower plates at the contact position are the same, the deformation equation of compatibility is expressed as:

$$
\begin{aligned}
&w_{m_1n_1}+2\left[\mu_{2m_1y_1}{b_1}^2\alpha_{m_1}^2\left(\frac{h_{n_1}}{\beta_{n_1}^4{b_1}^4}-\frac{\overline{h}_{n_1}}{90}\right)-\frac{h_{n_1}}{\beta_{n_1}^2{b_1}^2}+\frac{\overline{h}_{n_1}}{6}\right]C_{m_1}\\
&+2\left[\mu_{2m_1y_1}{b_1}^2\alpha_{m_1}^2\left(\frac{h_{n_1}}{\beta_{n_1}^4{b_1}^4}+\frac{7\overline{h}_{n_1}}{720}\right)-\frac{h_{n_1}}{\beta_{n_1}^2{b_1}^2}-\frac{\overline{h}_{n_1}}{12}\right](-1)^{n_1+1}D_{m_1}\\
&+2\left[\mu_{2m_1x_1}{a_1}^2\beta_{n_1}^2\left(\frac{h_{m_1}}{\alpha_{m_1}^4{a_1}^4}-\frac{\overline{h}_{m_1}}{90}\right)-\frac{h_{m_1}}{\alpha_{m_1}^2{a_1}^2}+\frac{\overline{h}_{m_1}}{6}\right]G_{n_1}\\
&+2\left[\mu_{2m_1x_1}{a_1}^2\beta_{n_1}^2\left(\frac{h_{m_1}}{\alpha_{m_1}^4{a_1}^4}+\frac{7\overline{h}_{m_1}}{720}\right)-\frac{h_{m_1}}{\alpha_{m_1}^2{a_1}^2}-\frac{\overline{h}_{m_1}}{12}\right](-1)^{m_1+1}H_{n_1}\\
&=\frac{4}{a_1b_1}\sum_{m_2=0}^{\infty}\sum_{n_2=0}^{\infty}\lambda_{m_2n_2}w_{m_2n_2}D+\frac{4}{a_1b_1}\sum_{m_2=0}^{\infty}\sum_{n_2=0}^{\infty}\lambda_{m_2n_2}D\cdot2\left[\mu_{2m_2y_2}{b_2}^2\alpha_{m_2}^2\left(\frac{h_{n_2}}{\beta_{n_2}^4{b_2}^4}-\frac{\overline{h}_{n_2}}{90}\right)-\frac{h_{n_2}}{\beta_{n_2}^2{b_2}^2}+\frac{\overline{h}_{n_2}}{6}\right]C_{m_2}\\
&+\frac{4}{a_1b_1}\sum_{m_2=0}^{\infty}\sum_{n_2=0}^{\infty}\lambda_{m_2n_2}D\cdot2\left[\mu_{2m_2y_2}{b_2}^2\alpha_{m_2}^2\left(\frac{h_{n_2}}{\beta_{n_2}^4{b_2}^4}+\frac{7\overline{h}_{n_2}}{720}\right)-\frac{h_{n_2}}{\beta_{n_2}^2{b_2}^2}-\frac{\overline{h}_{n_2}}{12}\right](-1)^{n_2+1}D_{m_2}\\
&+\frac{4}{a_1b_1}\sum_{m_2=0}^{\infty}\sum_{n_2=0}^{\infty}\lambda_{m_2n_2}D\cdot2\left[\mu_{2m_2x_2}{a_2}^2\beta_{n_2}^2\left(\frac{h_{m_2}}{\alpha_{m_2}^4{a_2}^4}-\frac{\overline{h}_{m_2}}{90}\right)-\frac{h_{m_2}}{\alpha_{m_2}^2{a_2}^2}+\frac{\overline{h}_{m_2}}{6}\right]G_{n_2}\\
&+\frac{4}{a_1b_1}\sum_{m_2=0}^{\infty}\sum_{n_2=0}^{\infty}\lambda_{m_2n_2}D\cdot2\left[\mu_{2m_2x_2}{a_2}^2\beta_{n_2}^2\left(\frac{h_{m_2}}{\alpha_{m_2}^4{a_2}^4}+\frac{7\overline{h}_{m_2}}{720}\right)-\frac{h_{m_2}}{\alpha_{m_2}^2{a_2}^2}-\frac{\overline{h}_{m_2}}{12}\right](-1)^{m_2+1}H_{n_2}\\
&(m_i=0,1,2,\cdots;\quad n_i=0,1,2,\cdots)
\end{aligned}
\tag{13}
$$

The double Fourier transformation of the ground reaction force is expressed as:

$$
Q(\xi,\eta)=-\frac{1}{2\pi}\sum_{m_2=0}^{\infty}\sum_{n_2=0}^{\infty}\lambda_{m_2n_2}Q_{m_2n_2}\frac{\left[e^{i\xi a}(-1)^{m_2}-1\right]\left[(-1)^{n_2}e^{i\eta b}-1\right]}{\xi\eta\left[1-(\frac{m_2\pi}{a\xi})^2\right]\left[1-(\frac{n_2\pi}{b\eta})^2\right]}
\tag{14}
$$

Expanding $w\big|_{z_2=0}$ into the double cosine series form:

$$
w\big|_{z_2=0}=\sum_{m_2=0}^{\infty}\sum_{n_2=0}^{\infty}\lambda_{m_2n_2}w_{z_2m_2n_2}\cos\frac{m_2\pi x_2}{a_2}\cos\frac{n_2\pi y_2}{b_2}
\tag{15}
$$

in which:

$$
w_{z_2m_2n_2}=\frac{4}{a_2b_2}\int_0^{a_2}\int_0^{b_2}w\big|_{z_2=0}\cos\frac{m_2\pi x_2}{a_2}\cos\frac{n_2\pi y_2}{b_2}dx_2dy_2
\tag{16}
$$

$$
w_{z_2m_2n_2}=\frac{1}{2\pi^2a_2b_2}\frac{(\lambda+2\mu)}{(\lambda+\mu)\mu}\sum_{p=0}^{\infty}\sum_{q=0}^{\infty}Q_{pq}\lambda_{pq}\eta_{pqm_2n_2}
\tag{17}
$$

where

$$
\eta_{pqm_2n_2}=\int_{-\infty}^{\infty}\int_{-\infty}^{\infty}\frac{1}{q_1}\frac{[(-1)^pe^{i\xi a}-1][(-1)^qe^{i\eta b}-1][(-1)^{m_2}e^{-i\xi a}-1][(-1)^{n_2}e^{-i\eta b}-1]}{\xi^2\eta^2\left[1-(\frac{m_2\pi}{a\xi})^2\right]\left[1-(\frac{n_2\pi}{b\eta})^2\right]\left[1-(\frac{p\pi}{a\xi})^2\right]\left[1-(\frac{q\pi}{b\eta})^2\right]}d\xi d\eta
$$

Equation (4) could be rewritten in a double cosine series form, and considering that the plate and surface of the elastic foundation have the same vertical displacement, thus

the coefficients of the corresponding items are also the same. The deformation equation of compatibility is given as:

$$\begin{aligned}
&\frac{1}{2\pi^2 a_2 b_2}\frac{(\lambda+2\mu)}{(\lambda+\mu)\mu}\sum_{p=0}^{\infty}\sum_{q=0}^{\infty}Q_{pq}\lambda_{pq}\eta_{pqm_2n_2}\lambda_{m_2n_2}\\
&=w_{m_2n_2}+2\left[\mu_{2m_2y_2}{b_2}^2\alpha_{m_2}^2\left(\frac{h_{n_2}}{\beta_{n_2}^4 b^4}-\frac{\bar{h}_{n_2}}{90}\right)-\frac{h_{n_2}}{\beta_{n_2}^2 {b_2}^2}+\frac{\bar{h}_{n_2}}{6}\right]C_{m_2}\\
&+2\left[\mu_{2m_2y_2}{b_2}^2\alpha_{m_2}^2\left(\frac{h_{n_2}}{\beta_{n_2}^4 {b_2}^4}+\frac{7\bar{h}_{n_2}}{720}\right)-\frac{h_{n_2}}{\beta_{n_2}^2 {b_2}^2}-\frac{\bar{h}_{n_2}}{12}\right](-1)^{n_2+1}D_{m_2}\\
&+2\left[\mu_{2m_2x_2}{a_2}^2\beta_{n_2}^2\left(\frac{h_{m_2}}{\alpha_{m_2}^4 {a_2}^4}-\frac{\bar{h}_{m_2}}{90}\right)-\frac{h_{m_2}}{\alpha_{m_2}^2 {a_2}^2}+\frac{\bar{h}_{m_2}}{6}\right]G_{n_2}\\
&+2\left[\mu_{2m_2x_2}{a_2}^2\beta_{n_2}^2\left(\frac{h_{m_2}}{\alpha_{m_2}^4 {a_2}^4}+\frac{7\bar{h}_{m_2}}{720}\right)-\frac{h_{m_2}}{\alpha_{m_2}^2 {a_2}^2}-\frac{\bar{h}_{m_2}}{12}\right](-1)^{m_2+1}H_{n_2}\\
&(m_i=0,1,2,\cdots;\quad n_i=0,1,2,\cdots)
\end{aligned}\tag{18}$$

Therefore, the undetermined coefficients $w_{m_1n_1}$, $F_{m_1n_1}$, C_{m_1}, D_{m_1}, G_{n_1}, H_{n_1}, $w_{m_2n_2}$, $Q_{m_2n_2}$, C_{m_2}, D_{m_2}, G_{n_2}, and H_{n_2} could be obtained by twelve equations (Equations (7)–(18)), in which N_1, N_2, M_1, and M_2 are the maximum values of n_1, n_2, m_1, and m_2, respectively. Thus, the number of the governing equation is $2(M_1 + 1)(N_1 + 1) + 2(M_1 + 1) + 2(N_1 + 1) + 2(M_2 + 1)(N_2 + 1) + 2(M_2 + 1) + 2(N_2 + 1)$, which can be used to solve the same number of undetermined coefficients. In order to ensure the correctness of the calculation results, the maximum values of M_1, M_2, N_1, and N_2 are taken to 20. Substituting the solved coefficients into Equation (1a,b), the deflection of the plate can be obtained, and further, the internal force and the foundation reaction can also be calculated.

2.1.3. Example

Case 1: We consider a stepped rectangular plate resting on the surface of an elastic half-space foundation. The dimensions of the upper and lower plates are 4.0 m × 0.2 m (side length × thickness) and 4 m × 0 m (side length × thickness), respectively, and the uniform load $q(x_1, y_1)$ on the plate is 0.98 MPa. In this case, the stepped rectangular plate degenerates into a rectangular plate. The performance parameters of the plate and the foundation are given in Table 1.

Table 1. Performance parameters.

	Poisson Ratio	Elastic Modulus (MPa)
Plate	0.167	34,300
Foundation	0.4	343

The subgrade reaction, bending moment, and deflection of the plate could be obtained by the solution, as shown in Figure 2.

Table 2 shows that the calculated results are consistent with the results in [28]. This comparison proves the effectiveness of the theory proposed in this paper.

Table 2. Comparison of calculation results of thin plate.

	In This Paper	[28]
Maximum deflection (m)	0.0107	0.0107
Maximum bending moment (kN·m)	35.558	35.558

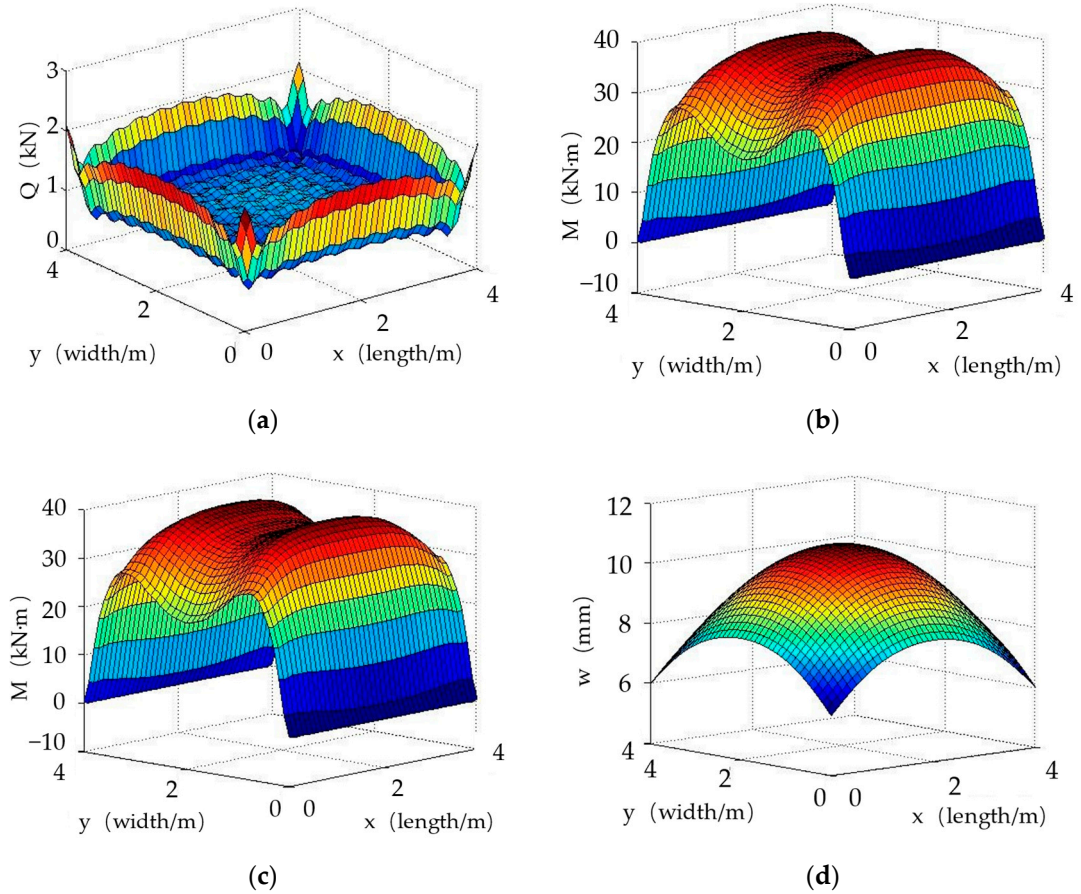

Figure 2. Calculation results using thin plate theory: (**a**) Subgrade reaction; (**b**) Bending moment of the plate (M_y); (**c**) Bending moment of the plate (M_x); (**d**) Deflection of the plate.

Case 2: We consider a stepped rectangular plate resting on the surface of an elastic half-space foundation. The dimensions of the upper and lower plates are 4.0 m × 0.2 m (side length × thickness) and 4 m × 0.2 m (side length × thickness), respectively, and the concentrated loading on the plate is F = 100 kN. The performance parameters of the stepped plate and the foundation are given in Table 3.

Table 3. Performance parameters of the stepped rectangular plate.

Component Name	Poisson Ratio	Elastic Modulus (MPa)
Upper plate	0.167	26,000
Lower plate	0.167	26,000
Foundation	0.4	343

Figure 3 shows the comparison of the analytical solution and the simulation results, in which the model is created by ABAQUS software. For the deflection at the center of the lower plate, the result of the finite element model is smaller than that of the analytical solution when it is close to the edge of the plate, while when it is close to the center of the plate, the situation is just the opposite (Figure 3a). For the bending moment of the lower plate at x = 0.5 m and y = 0.5 m, the curve increases slowly at the edge of the plate, and as it approaches the center of the plate, the curve increases first and then decreases (Figure 3b,c). It can be concluded that the results of finite element model well support the present results using the thin plate theory.

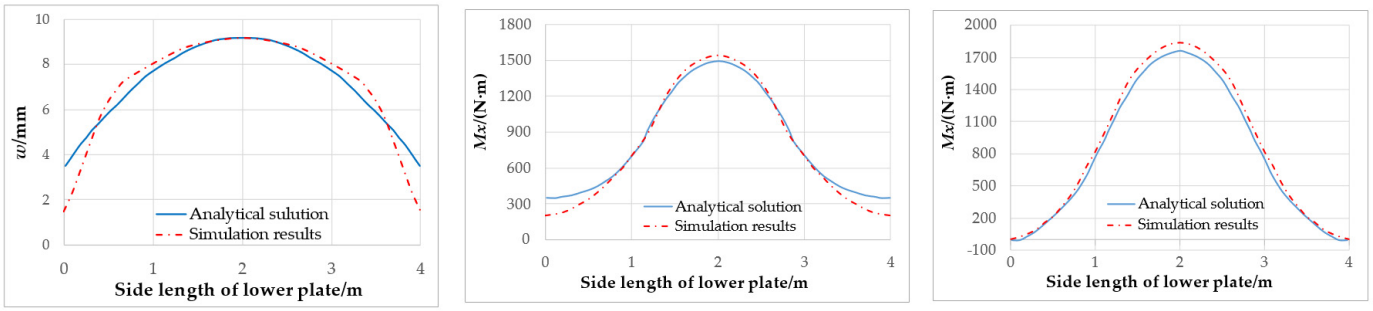

(**a**) (**b**) (**c**)

Figure 3. Verification of finite element software: (**a**) Deflection at the center of the lower plate; (**b**) Bending moment of the lower plate at x = 0.25 m (M_x); (**c**) Bending moment of the lower plate at y = 0.25 m (M_x).

2.2. Both Upper and Lower Parts of the Plate Are Moderately Thick Plates

2.2.1. Basic Equations and Boundary Conditions

The governing differential equations of the moderately thick plate are determined by formulas [27]:

$$D_{11}\frac{\partial^2\Phi_{x_1}}{\partial {x_1}^2}+D_{66}\frac{\partial^2\Phi_{x_1}}{\partial {y_1}^2}+(D_{12}+D_{66})\frac{\partial^2\Phi_{y_1}}{\partial x_1\partial y_1}+C_{11}\frac{\partial w_1}{\partial x_1}-C_{11}\Phi_{x_1}=0$$

$$D_{22}\frac{\partial^2\Phi_{y_1}}{\partial {y_1}^2}+D_{66}\frac{\partial^2\Phi_{y_1}}{\partial {x_1}^2}+(D_{12}+D_{66})\frac{\partial^2\Phi_{x_1}}{\partial x_1\partial y_1}+C_{22}\frac{\partial w_1}{\partial y_1}-C_{22}\Phi_{y_1}=0$$

$$C_{11}\frac{\partial^2 w_1}{\partial {x_1}^2}+C_{22}\frac{\partial^2 w_1}{\partial {y_1}^2}-C_{11}\frac{\partial\Phi_{x_1}}{\partial x_1}-C_{22}\frac{\partial\Phi_{y_1}}{\partial y_1}+q-F=0$$

$$D_{11}\frac{\partial^2\Phi_{x_2}}{\partial {x_2}^2}+D_{66}\frac{\partial^2\Phi_{x_2}}{\partial {y_2}^2}+(D_{12}+D_{66})\frac{\partial^2\Phi_{y_2}}{\partial x_2\partial y_2}+C_{11}\frac{\partial w_2}{\partial x_2}-C_{11}\Phi_{x_2}=0$$

$$D_{22}\frac{\partial^2\Phi_{y_2}}{\partial {y_2}^2}+D_{66}\frac{\partial^2\Phi_{y_2}}{\partial {x_2}^2}+(D_{12}+D_{66})\frac{\partial^2\Phi_{x_2}}{\partial x_2\partial y_2}+C_{22}\frac{\partial w_2}{\partial y_2}-C_{22}\Phi_{y_2}=0$$

$$C_{11}\frac{\partial^2 w_2}{\partial {x_2}^2}+C_{22}\frac{\partial^2 w_2}{\partial {y_2}^2}-C_{11}\frac{\partial\Phi_{x_2}}{\partial x_2}-C_{22}\frac{\partial\Phi_{y_2}}{\partial y_2}+F-Q=0$$

where Φ_{x_i}, Φ_{y_i}, w_i, F, Q are unknown coefficients.

Boundary restrictions are given as:

$$M_{x_i}=M_{x_iy_i}=Q_{x_i}=0(x_i=0,x_i=\mathrm{a})$$

$$M_{y_i}=M_{x_iy_i}=Q_{y_i}=0(y_i=0,y_i=\mathrm{b})$$

2.2.2. Coordination Equation and Analytical Solution

Expanding Φ_{x_i}, Φ_{y_i}, w_i, F, Q, q into a Fourier series

$$\Phi_{x_i}=\sum_{m_i}\sum_{n_i}\varphi_{m_in_i}\sin\alpha_{m_i}x_i\cos\beta_{n_i}y_i$$

$$\Phi_{y_i}=\sum_{m_i}\sum_{n_i}\psi_{m_in_i}\cos\alpha_{m_i}x_i\sin\beta_{n_i}y_i$$

$$w_i=\sum_{m_i}\sum_{n_i}w_{m_in_i}\cos\alpha_{m_i}x_i\cos\beta_{n_i}y_i$$

$$F = \sum_{m_2}\sum_{n_2} F_{m_2n_2}\cos\alpha_{m_2}x_2\cos\beta_{n_2}y_2$$

$$Q = \sum_{m_i}\sum_{n_i} Q_{m_in_i}\cos\alpha_{m_i}x_i\cos\beta_{n_i}y_i$$

$$q = \sum_{m_1}\sum_{n_1} q_{m_1n_1}\cos\alpha_{m_1}x_1\cos\beta_{n_1}y_1$$

in which $\Phi_{m_in_i}$, $\psi_{m_in_i}$, $w_{m_in_i}$, $F_{m_2n_2}$, $q_{m_1n_1}$ and $Q_{m_in_i}$ are unknown coefficients.

Taking into account the continuous differentiability of the formula on the boundary of the plate, we can write:

$$\frac{\partial w_i(0,y_i)}{\partial x_i} = -\frac{a_i}{4}\sum_{n_i} a_{n_i}\cos\beta_{n_i}y_i; \frac{\partial w_i(x_i,0)}{\partial y_i} = -\frac{b_i}{4}\sum_{n_i} b_{m_i}\cos\alpha_{m_i}x_i$$

$$\Phi_{x_i}(0,y_i) = -\frac{a_i}{4}\sum_{n_i} c_{n_i}\cos\beta_{n_i}y_i; \Phi_{y_i}(x_i,0) = -\frac{b_i}{4}\sum_{n_i} d_{m_i}\cos\alpha_{m_i}x_i$$

$$\frac{\partial w_i(a_i,y_i)}{\partial x_i} = -\frac{a_i}{4}\sum_{n_i} e_{n_i}\cos\beta_{n_i}y_i; \frac{\partial w_i(x_i,b_i)}{\partial y_i} = -\frac{b_i}{4}\sum_{n_i} f_{m_i}\cos\alpha_{m_i}x_i$$

$$\Phi_{x_i}(a_i,y_i) = -\frac{a_i}{4}\sum_{n_i} g_{n_i}\cos\beta_{n_i}y_i; \Phi_{y_i}(x_i,b_i) = -\frac{b_i}{4}\sum_{n_i} h_{m_i}\cos\alpha_{m_i}x_i$$

where a_{n_i}, b_{m_i}, c_{n_i}, d_{m_i}, e_{n_i}, f_{m_i}, g_{n_i}, and h_{m_i} are unknown coefficients. According to boundary conditions, we obtain the expressions:

$$a_{n_i} = c_{n_i},\ e_{n_i} = g_{n_i},\ b_{m_i} = d_{m_i},\ f_{m_i} = h_{m_i}$$

(1) Derived from $M_{x_i} = 0$ on the edge $x_i = 0$, we obtain the expression:

$$\sum_{m_i}\left[\frac{\varepsilon_{m_i}}{2}D_{11}(e_{n_i}\cos m_i\pi - a_{n_i}) - \alpha_{m_i}\varphi_{m_in_i}D_{11} + \frac{\varepsilon_{m_i}}{2}(f_{m_i}\cos m_i\pi - b_{m_i})D_{12} - \beta_{n_i}\psi_{m_in_i}D_{12}\right] = 0$$

(2) Derived from $M_{x_i} = 0$ on the edge $x_i = a_i$, we obtain the expression:

$$\sum_{m_i}\left[\frac{\varepsilon_{m_i}}{2}D_{11}(e_{n_i}\cos m_i\pi - a_{n_i}) - \alpha_{m_i}\varphi_{m_in_i}D_{11} + \frac{\varepsilon_{m_i}}{2}(f_{m_i}\cos m_i\pi - b_{m_i})D_{12} - \beta_{n_i}\psi_{m_in_i}D_{12}\right]\cos\alpha_{m_i}a_i = 0$$

(3) Derived from $M_{y_i} = 0$ on the edge $y_i = 0$, we obtain the expression:

$$\sum_{n_i}\left[\frac{\varepsilon_{m_i}}{2}D_{12}(e_{n_i}\cos m_i\pi - a_{n_i}) - \alpha_{m_i}\varphi_{m_in_i}D_{12} + \frac{\varepsilon_{m_i}}{2}(f_{m_i}\cos m_i\pi - b_{m_i})D_{22} - \beta_{n_i}\psi_{m_in_i}D_{22}\right] = 0$$

(4) Derived from $M_{y_i} = 0$ on the edge $y_i = b_i$, we obtain the expression:

$$\sum_{n_i}\left[\frac{\varepsilon_{m_i}}{2}D_{12}(e_{n_i}\cos m_i\pi - a_{n_i}) - \alpha_{m_i}\varphi_{m_in_i}D_{12} + \frac{\varepsilon_{m_i}}{2}(f_{m_i}\cos m_i\pi - b_{m_i})D_{22} - \beta_{n_i}\psi_{m_in_i}D_{22}\right]\cos\beta_{n_i}b_i = 0$$

Substituting the unfolded Fourier form of Φ_{x_i}, Φ_{y_i}, and w into the governing differential equations, the expressions can be written as:

$$\begin{aligned}
&\tfrac{\alpha_{m_1}\varepsilon_{m_1}}{2}D_{11}a_{n_1} + \tfrac{\alpha_{m_1}\varepsilon_{n_1}}{2}D_{12}b_{m_1} - \tfrac{\alpha_{m_1}\varepsilon_{m_1}}{2}D_{11}\cos m_1\pi e_{n_1} - \tfrac{\alpha_{m_1}\varepsilon_{n_1}}{2}D_{12}\cos n_1\pi f_{m_1}\\
&+\left(D_{11}\alpha_{m_1}^2 + D_{66}\beta_{n_1}^2 + C_{11}\right)\varphi_{m_1n_1} + (D_{12}+D_{66})\alpha_{m_1}\beta_{n_1}\psi_{m_1n_1} + \alpha_{m_1}C_{11}w_{m_1n_1} = 0\\
&\tfrac{\beta_{n_1}\varepsilon_{m_1}}{2}D_{12}a_{n_1} + \tfrac{\beta_{n_1}\varepsilon_{n_1}}{2}D_{22}b_{m_1} - \left(\tfrac{\beta_{n_1}\varepsilon_{m_1}}{2}D_{12}\cos m_1\pi\right)e_{n_1} - \left(\tfrac{\beta_{n_1}\varepsilon_{n_1}}{2}D_{22}\cos n_1\pi\right)f_{m_1}\\
&+\alpha_{m_1}\beta_{n_1}(D_{12}+D_{66})\varphi_{m_1n_1} + \left(\beta_{n_1}^2D_{22} + \alpha_{m_1}^2D_{66} + C_{22}\right)\psi_{m_1n_1} + \beta_{n_1}C_{22}w_{m_1n_1} = 0
\end{aligned}$$

$$\alpha_{m_1}C_{11}\varphi_{m_1n_1}+\beta_{n_1}C_{22}\psi_{m_1n_1}+\left(\alpha_{m_1}^2C_{11}+\beta_{n_1}^2C_{22}\right)w_{m_1n_1}+F_{m_1n_1}=q_{m_1n_1}$$

$$\begin{aligned}&\tfrac{\alpha_{m_2}\varepsilon_{m_2}}{2}D_{11}a_{n_2}+\tfrac{\alpha_{m_2}\varepsilon_{n_2}}{2}D_{12}b_{m_2}-\tfrac{\alpha_{m_2}\varepsilon_{m_2}}{2}D_{11}\cos m_2\pi e_{n_2}-\tfrac{\alpha_{m_2}\varepsilon_{n_2}}{2}D_{12}\cos n_2\pi f_{m_2}\\&+\left(D_{11}\alpha_{m_2}^2+D_{66}\beta_{n_2}^2+C_{11}\right)\varphi_{m_2n_2}+(D_{12}+D_{66})\alpha_{m_2}\beta_{n_2}\psi_{m_2n_2}+\alpha_{m_2}C_{11}w_{m_2n_2}=0\end{aligned}$$

$$\begin{aligned}&\tfrac{\beta_{n_2}\varepsilon_{m_2}}{2}D_{12}a_{n_2}+\tfrac{\beta_{n_2}\varepsilon_{n_2}}{2}D_{22}b_{m_2}-\left(\tfrac{\beta_{n_2}\varepsilon_{m_2}}{2}D_{12}\cos m_2\pi\right)e_{n_2}-\left(\tfrac{\beta_{n_2}\varepsilon_{n_2}}{2}D_{22}\cos n_2\pi\right)f_{m_2}\\&+\alpha_{m_2}\beta_{n_2}(D_{12}+D_{66})\varphi_{m_2n_2}+\left(\beta_{n_2}^2D_{22}+\alpha_{m_2}^2D_{66}+C_{22}\right)\psi_{m_2n_2}+\beta_{n_2}C_{22}w_{m_2n_2}=0\end{aligned}$$

$$\alpha_{m_2}C_{11}\varphi_{m_2n_2}+\beta_{n_2}C_{22}\psi_{m_2n_2}+\left(\alpha_{m_2}^2C_{11}+\beta_{n_2}^2C_{22}\right)w_{m_2n_2}+Q_{m_2n_2}=F_{m_2n_2}$$

Considering the same displacement of the upper and lower plates at the contacting position, thus, the deflection equations of the upper and lower plates could be expanded into a double cosine series as:

$$\begin{aligned}&w_i(x_i,y_i)=\sum_{m_i=0}^{\infty}\sum_{n_i=0}^{\infty}\lambda_{m_in_i}w_{im_in_i}\cos\tfrac{m_i\pi x_i}{a_i}\cos\tfrac{n_i\pi y_i}{b_i}\\&w_{im_in_i}=\tfrac{4}{a_ib_i}\int_0^{b_i}\int_0^{a_i}w_i(x_i,y_i)\cos\tfrac{m_i\pi x_i}{a_i}\cos\tfrac{n_i\pi y_i}{b_i}dx_idy_i\\&w_{2m_1n_1}=\tfrac{4}{a_1b_1}\int_0^{b_1}\int_0^{a_1}W_2(x_2,y_2)\cos\tfrac{m_1\pi x_1}{a_1}\cos\tfrac{n_1\pi y_1}{b_1}dx_1dy_1\\&=\tfrac{4}{a_1b_1}\int_0^{b_1}\int_0^{a_1}\sum_{m_2=0}^{\infty}\sum_{n_2=0}^{\infty}\lambda_{m_2n_2}w_{2m_2n_2}\cos\tfrac{m_1\pi x_1}{a_1}\cos\tfrac{n_1\pi y_1}{b_1}\cos\tfrac{m_2\pi x_2}{a_2}\cos\tfrac{n_2\pi y_2}{b_2}dx_1dy_1\\&=\tfrac{4}{a_1b_1}\sum_{m_2=0}^{\infty}\sum_{n_2=0}^{\infty}\lambda_{m_2n_2}w_{2m_2n_2}\int_0^{b_1}\int_0^{a_1}\cos\tfrac{m_1\pi x_1}{a_1}\cos\tfrac{n_1\pi y_1}{b_1}\cos\tfrac{m_2\pi x_2}{a_2}\cos\tfrac{n_2\pi y_2}{b_2}dx_1dy_1\\&=\tfrac{4}{a_1b_1}\sum_{m_2=0}^{\infty}\sum_{n_2=0}^{\infty}\lambda_{m_2n_2}w_{2m_2n_2}\int_0^{b_1}\int_0^{a_1}\cos\tfrac{m_1\pi x_1}{a_1}\cos\tfrac{n_1\pi y_1}{b_1}\cos\tfrac{m_2\pi(x_1+x_0)}{a_2}\cos\tfrac{n_2\pi(y_1+y_0)}{b_2}dx_1dy_1\\&=\tfrac{4}{a_2b_2}\sum_{m_2=0}^{\infty}\sum_{n_2=0}^{\infty}\lambda_{m_2n_2}w_{m_2n_2}D\\&(m_i=0,1,2,\cdots;\quad n_i=0,1,2,\cdots)\end{aligned}$$

The deformation coordination equation between the upper and the lower plates is expressed as:

$$w_{1m_1n_1}=\frac{4}{a_1b_1}\sum_{m_2=0}^{\infty}\sum_{n_2=0}^{\infty}\lambda_{m_2n_2}w_{2m_2n_2}D$$

The deformation coordination equation between the lower plate and the foundation is given as:

$$\frac{1}{2\pi^2a_2b_2}\frac{(\lambda+2\mu)}{(\lambda+\mu)\mu}\sum_{p=0}^{\infty}\sum_{q=0}^{\infty}Q_{pq}\lambda_{pq}\eta_{pqm_2n_2}\lambda_{m_2n_2}=w_{m_2n_2}$$

Using the same method in Section 2.1, the undetermined coefficients a_{n_i}, b_{m_1}, e_{n_1}, f_{m_1}, $\varphi_{m_in_i}$, $\psi_{m_in_i}$, $w_{m_in_i}$, $F_{m_in_i}$, and $Q_{m_2n_2}$ could be simultaneously solved. Substituting the solved coefficients into related formulas, the subgrade reaction, deflection, and internal force of the plate could be obtained.

2.2.3. Example

Case 3: Recalculating case 1 in Section 2.1.3. According to the theory mentioned in this section, the results are given in Figure 4. Through the comparison of Figures 2 and 4, it can be seen that the subgrade reaction, deflection, and internal force of the plate are basically the same.

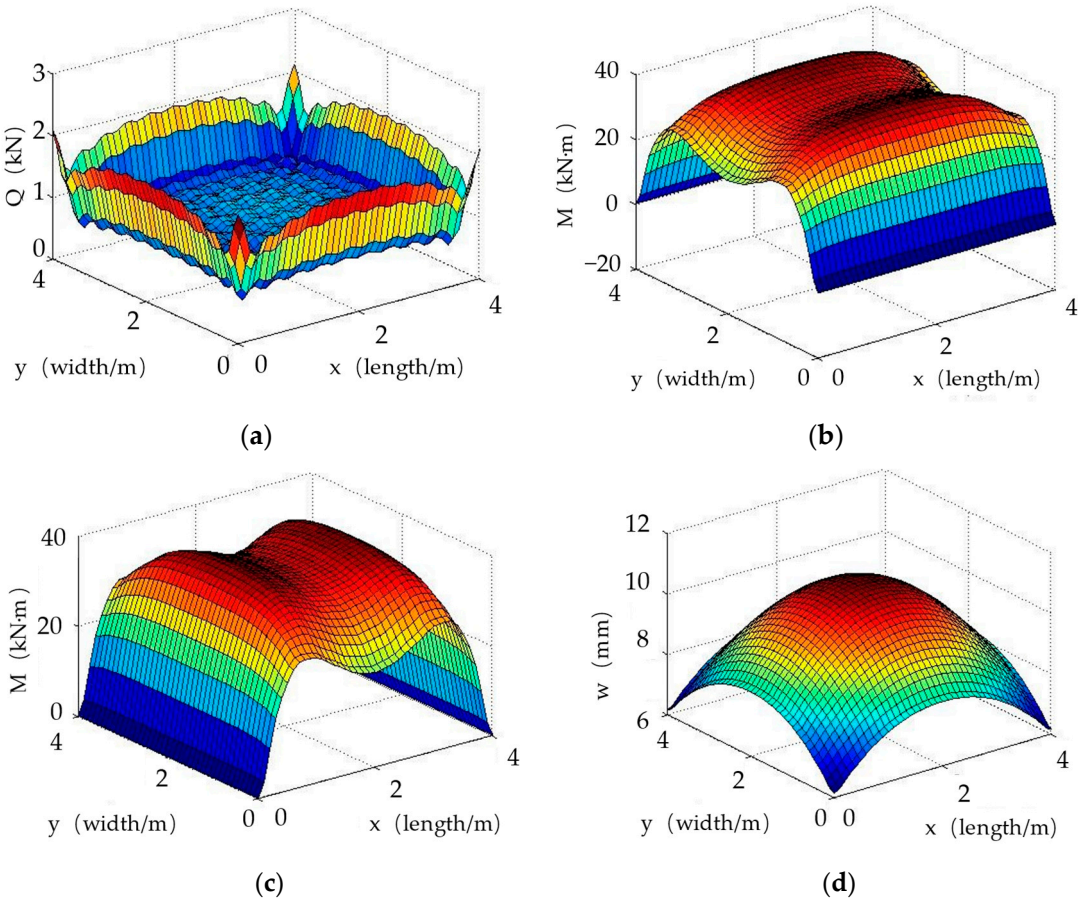

Figure 4. Calculation results using thick plate theory: (**a**) Subgrade reaction; (**b**) Bending moment of plate (M_y); (**c**) Bending moment of plate (M_x); (**d**) Deflection of plate.

Meanwhile, the analytical solution in this paper is consistent with the results in [28], as shown in Table 4. This comparison proves the effectiveness of the theory proposed in this paper.

Table 4. Comparison of calculation results of thick plate.

	In This Paper	Thin Plate Theory	[28]
Maximum deflection (m)	0.0107	0.0107	0.0107
Maximum bending moment (kN·m)	35.551	35.558	35.558

Case 4: The recalculated results of case 2 in Section 2.1.3 also indicate that the influence of plate theory on the internal force and deflection of the plate is relatively small. Due to the limited length of this article, the specific curve is no longer listed.

When the stepped rectangular plate is simultaneously analyzed using both moderately thick plate theory and thin plate theory, the same method (as shown in Sections 2.1 and 2.2) could be used to obtain the internal force and deflection of the stepped rectangular plate.

3. Discussion

3.1. Effect of Elastic Modulus on the Deflection of Plate

The dimensions, Poisson ratios, and elastic modulus of the rectangular stepped plate and foundation are given in Table 5. The vertical uniform load value is 0.98 MPa. The deflection curve of the center line of the plate is shown in Figure 5, in which the number of

the curves 1, 2, 3, and 4 indicate that the elastic modulus of the upper plate is 34,300 MPa, 343,000 MPa, 686,000 MPa, and 1,029,000 MPa, respectively.

Table 5. Dimensions and properties of plates with different elastic modulus.

Component Name	Side Length (m)	Thickness (m)	Poisson Ratio	Elastic Modulus (MPa)
Upper plate	2.0	0.1	0.167	Variable
Lower plate	4.0	0.3	0.167	34,300
Foundation	-	-	0.4	343

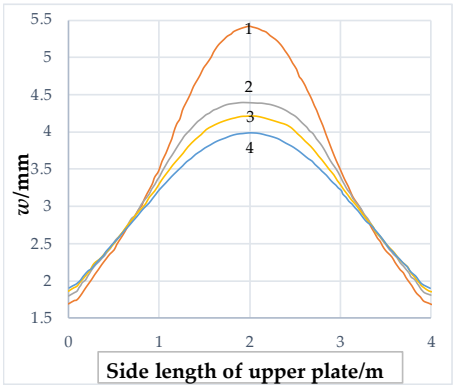

Figure 5. Deflection curve of lower plates with different elastic modulus.

Through the analysis of Figure 5, it can be seen that the variation trend of the deflection curve of the lower plate is the same as that of Figure 3a. The deflection value of the lower plate is largest when the elastic modulus of the upper and lower plates is the same. The deflection along the center line of the plate decreases with the increase of the elastic modulus of the upper plate, while the deflection at the edge of the plate is just the opposite.

3.2. Influence of Plate Theory on Calculation Results of Plate Deflection

The dimensions, Poisson ratios, and elastic modulus of the rectangular stepped plate and foundation are given in Table 6. The vertical uniform load value is 0.98 MPa, and the thickness of the lower plate is 0.2 m, 0.3 m, 0.4 m, 0.5 m, 0.6 m, 0.7 m, 0.8 m, 0.9 m, and 1.0 m, respectively. The deflection of the center of the lower plate is given in Table 7, in which w_1 and w_2 are the deflection values calculated by thin plate theory and moderately thick plate theory, respectively.

Table 6. Dimensions and properties of plates with different thickness.

Component Name	Side Length (m)	Thickness (m)	Poisson Ratio	Elastic Modulus (MPa)
Upper plate	2.0	0.2	0.167	34,300
Lower plate	2.0	Variable	0.167	34,300
Foundation	-	-	0.4	343

Through the calculation results in Table 7, it can be obtained that when the thickness of the upper plate is constant, the maximum deflection of the lower plate decreases with the increase in the thickness. Meanwhile, the comparison of w_1 and w_2 shows that the plate theory has little influence on the analytical solution of the maximum deflection of the plate.

Table 7. Deflection at the center of the lower plate.

Thickness of Lower Plate (m)	w_1 (m)	w_2 (m)
0.2	0.0053	0.0052
0.3	0.0042	0.0041
0.4	0.0035	0.0034
0.5	0.0030	0.0030
0.6	0.0027	0.0027
0.7	0.0025	0.0025
0.8	0.0024	0.0024
0.9	0.0023	0.0023
1.0	0.0022	0.0023

3.3. Influence of Side Length of Upper and Lower Plates on Calculation Results of Plate Deflection

The dimensions of the stepped rectangular plates are given in Table 8. The vertical uniform load value is 0.98 MPa. Calculation results can be seen in Figure 6, in which 1, 2, 3, and 4 indicate the side lengths of the upper plate are 3.0 m, 2.0 m, 1.0 m, and 0.5 m, respectively.

Table 8. Dimensions and properties of plates with different side length.

Component Name	Side Length (m)	Thickness (m)	Poisson Ratio	Elastic Modulus (MPa)
Upper plate	Variable	0.2	0.167	34,300
Lower plate	4.0	0.3	0.167	34,300
Foundation	-	-	0.4	343

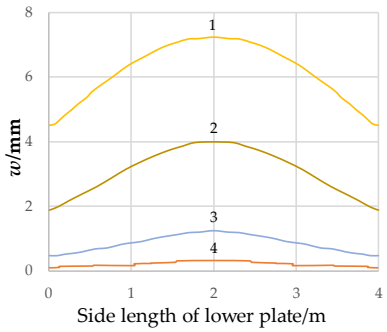

Figure 6. Deflection curve of lower plates with different side length.

It can be seen from Figure 6 that the deflection of the center of the plate increases as the size of the upper plate increases. It can also be found that when the coordinates of x are between 0–1 or 3–4, the deflection growth rate is relatively fast, while the growth rate of deflection is slow when $2 < x < 4$, indicating that the existence of the upper plate increases the stiffness of the lower plate.

4. Conclusions

This paper presents a new solving method to obtain the bending moment and deflection of the stepped rectangular plate using traditional thin plate theory and moderately thick plate theory. The stepped rectangular plate is divided into an upper plate and lower plate, and the analytical solution could be obtained through the differential equation and boundary conditions of the plate-foundation system. Several conclusions can be drawn as follows.

(1) The analytical solution is basically the same as those in the existing literature and the simulation results using ABAQUS software, indicating that the traditional plate theory could be used to analyze the bending property of stepped rectangular plate. The

analysis results also demonstrate that the analytical solution of the stepped rectangular plate is not related to the plate theory adopted.

(2) The increase in the elastic modulus of the upper plate can effectively reduce the deflection at the center of the plate and slightly increase the deflection at the edge of the plate, showing that the increase in the elastic modulus of the upper plate could effectively improve the stiffness of the stepped rectangular plate.

(3) The thickness and maximum deflection of the plate are negatively related when the thin plate theory or moderately thick plate theory is used for analysis, and the analytical solution obtained by using these two types of plate theory is basically the same.

(4) The greater the difference in the side length of the upper and lower plates, the greater the deflection of the stepped rectangular plate. The increase in the deflection at the edge of the plate is not as significant as that at the center of the plate.

Due to the limitations of time, level, and vision, the research on the topics of this paper is not yet complete. In the future, more in-depth research can be conducted regarding the following aspects:

(1) The interaction between the plate and the elastic half-space foundation is discussed in this paper, but the characteristics of the stepped rectangular plate resting on a two-parameter foundation should be analyzed in the future.

(2) The bending performance of the plate resting on an elastic half-space foundation under static load is analyzed in this paper, while the dynamic characteristics of the plate should be studied in future research.

(3) The characteristics of the stepped rectangular plate embedded in the foundation should be studied in follow-up research.

Author Contributions: Conceptualization, J.W. and X.L.; methodology, X.L.; software, J.Z.; validation, J.W. and X.L.; formal analysis, X.L.; investigation, X.L.; resources, J.W.; data curation, J.Z.; writing—original draft preparation, J.W. and X.L.; writing—review and editing, J.Z.; visualization, J.Z.; supervision, J.W.; project administration, J.W.; funding acquisition, J.W. All authors have read and agreed to the published version of the manuscript.

Funding: This research was supported by the Natural Science Foundation of Shaanxi Province (2021JQ-876) and Scientific Research Foundation for High-level Talents (XJ17T08). The authors would like to thank Shaanxi Key Laboratory of Safety and Durability of Concrete Structures for the project testing.

Data Availability Statement: Data sharing is not applicable to this article.

Conflicts of Interest: The authors declare no conflict of interest.

Appendix A

The deflection of the plate could be expressed using a double cosine series

$$w = \Phi(x,y) + \Phi_1(x,y) + \Phi_2(x,y) \tag{A1}$$

in which $\Phi(x,y)$ is the double cosine series, $\Phi_1(x,y)$ and $\Phi_2(x,y)$ are the cosine series of x and y, respectively.

$$\Phi(x,y) = \sum_{m=0}^{\infty}\sum_{n=0}^{\infty} w_{mn}\cos\tfrac{m\pi x}{a}\cos\tfrac{n\pi x}{b}$$
$$\Phi_1(x,y) = \sum_{m=0}^{\infty}(A_{1m}y^4 + B_{1m}y^3 + C_{1m}y^2 + D_{1m}y)\cos\tfrac{m\pi x}{a}$$
$$\Phi_2(x,y) = \sum_{n=0}^{\infty}(A_{2n}x^4 + B_{2n}x^3 + C_{2n}x^2 + D_{1n}x)\cos\tfrac{n\pi y}{b}$$

where A_{1m}~D_{1m} and A_{2n}~D_{2n} are undetermined parameters.

The shear force and rotating angle along the four sides of the plate are expressed by the cosine series.

$$F_{sy}(x,0) = \sum_{m=0}^{\infty} \frac{1}{b} A_m \cos\frac{m\pi x}{a}, F_{sy}(x,b) = \sum_{m=0}^{\infty} \frac{1}{b} B_m \cos\frac{m\pi x}{a} \tag{A2}$$

$$\theta_y(x,0) = \sum_{m=0}^{\infty} \frac{1}{b} C_m \cos\frac{m\pi x}{a}, \theta_y(x,b) = \sum_{m=0}^{\infty} \frac{1}{b} D_m \cos\frac{m\pi x}{a} \tag{A3}$$

$$F_{sx}(0,y) = \sum_{n=0}^{\infty} \frac{1}{a} E_n \cos\frac{n\pi y}{b}, F_{sx}(a,y) = \sum_{n=0}^{\infty} \frac{1}{a} F_n \cos\frac{n\pi y}{b} \tag{A4}$$

$$\theta_x(0,y) = \sum_{n=0}^{\infty} \frac{1}{a} G_n \cos\frac{n\pi y}{b}, \theta_x(a,y) = \sum_{n=0}^{\infty} \frac{1}{a} H_n \cos\frac{n\pi y}{b} \tag{A5}$$

in which A_m~D_m and E_n~H_n are undetermined parameters.

The total shear force could be written as

$$\frac{\partial^3 w}{\partial^3 y} + \mu_{2my}\frac{\partial^3 w}{\partial y \partial^2 x} = \frac{F_{sy}}{D_y}, \frac{\partial^3 w}{\partial^3 x} + \mu_{2mx}\frac{\partial^3 w}{\partial x \partial^2 y} = \frac{F_{sx}}{D_x} \tag{A6}$$

where $\mu_{2my} = \frac{H_y + 2D_{x_i y_i}}{D_{y_i}}$, $\mu_{2mx} = \frac{H_x + 2D_{x_i y_i}}{D_{x_i}}$, D_x and D_y are the bending stiffness of x-axial and y-axial direction, respectively.

With account of Equations (A1)–(A6), A_{1m}~D_{2m} and A_{1n}~D_{2n} could be represented by A_m~D_m and E_n~H_n. Equation (A1) could be rewritten as:

$$\begin{aligned} w_i = {} & \sum_{m=0}^{\infty}\sum_{n=0}^{\infty} w_{mn}\cos\tfrac{m\pi x}{a}\cos\tfrac{n\pi y}{b} + \sum_{m=0}^{\infty}\left\{\left[\mu_{2my}\tfrac{m^2\pi^2 b^2}{a^2}\cdot\tfrac{(D_m - C_m)}{24b^2} + \tfrac{A_m - B_m}{24b^2 D_y}\right]y^4 + \right. \\ & + \left(\mu_{2my}\cdot\tfrac{m^2\pi^2 b^2}{a^2}\cdot\tfrac{C_m}{6b} - \tfrac{A_m}{6bD_y}\right)y^3 - \left[\tfrac{(3+\mu_{2my}\cdot b^2\cdot\frac{m^2\pi^2 b^2}{a^2})C_m}{6b^2} - \tfrac{(6-\mu_{2my}\cdot b^2\cdot\frac{m^2\pi^2 b^2}{a^2})D_m}{12b^2}\right. \\ & \left. - \tfrac{2A_m + B_m}{12bD_y}\right]y^2 + \tfrac{C_m}{b}y\Big\}\cos\tfrac{m\pi x}{a} + \sum_{n=0}^{\infty}\left\{\left[\mu_{2mx}\tfrac{m^2\pi^2 a^2}{b^2}\cdot\tfrac{(H_n - G_n)}{24a^2} + \tfrac{E_n - F_n}{24a^2 D_x}\right]x^4 + \right. \\ & + \left(\mu_{2mx}\cdot\tfrac{m^2\pi^2 a^2}{b^2}\cdot\tfrac{G_n}{6a} - \tfrac{E_n}{6aD_x}\right)x^3 - \left[\tfrac{(3+\mu_{2mx}\cdot a^2\cdot\frac{m^2\pi^2 a^2}{b^2})G_n}{6a^2} - \tfrac{(6-\mu_{2mx}\cdot a^2\cdot\frac{m^2\pi^2 a^2}{b^2})H_n}{12a^2}\right. \\ & \left. \left. - \tfrac{2E_n + F_n}{12aD_x}\right]x^2 + \tfrac{G_n}{a}x\right\}\cos\tfrac{n\pi x}{b} \end{aligned} \tag{A7}$$

If the four sides of the plate are free and considering that the stepped plate is divided into lower and upper plates, it can be known that $A_m = B_m = E_n = F_n = 0$. Therefore, Equation (A7) can be expressed as:

$$\begin{aligned} w_i = {} & \sum_{m_i=0}^{\infty}\sum_{n_i=0}^{\infty} w_{m_i n_i}\cos\tfrac{m_i\pi x_i}{a_i}\cos\tfrac{n_i\pi y_i}{b_i} + \sum_{m_i=0}^{\infty}\left\{\left[\mu_{2m_i y_i}\tfrac{{m_i}^2\pi^2{b_i}^2}{{a_i}^2}\cdot\tfrac{4b_i{y_i}^3 - 4{b_i}^2{y_i}^2 - {y_i}^4}{24{b_i}^4}\right.\right. \\ & \left. + \tfrac{2b_i y_i - {y_i}^2}{2{b_i}^2}\right]C_{m_i} + \left[\mu_{2m_i y_i}\tfrac{{m_i}^2\pi^2{b_i}^2}{{a_i}^2}\cdot\tfrac{{y_i}^4 - 2{b_i}^2{y_i}^2}{24{b_i}^4} + \tfrac{{y_i}^2}{2{b_i}^2}\right]D_{m_i}\Big\}\cos\tfrac{m_i\pi x_i}{a_i} \\ & + \sum_{n_i=0}^{\infty}\left\{\left[\mu_{2m_i x_i}\tfrac{{n_i}^2\pi^2{a_i}^2}{{b_i}^2}\cdot\tfrac{4a_i{x_i}^3 - 4{a_i}^2{x_i}^2 - {x_i}^4}{24{a_i}^4} + \tfrac{2a_i x_i - {x_i}^2}{2{a_i}^2}\right]G_{n_i} + \left[\mu_{2m_i x_i}\tfrac{{n_i}^2\pi^2{a_i}^2}{{b_i}^2}\right.\right. \\ & \left.\left.\cdot\tfrac{{x_i}^4 - 2{a_i}^2{x_i}^2}{24{a_i}^4} + \tfrac{{x_i}^2}{2{a_i}^2}\right]H_{n_i}\right\}\cos\tfrac{n_i\pi y_i}{b_i} \end{aligned}$$

References

1. Kotousov, A. Effect of plate thickness on stress state at sharp notches and the strength paradox of thick plates. *Int. J. Solids Struct.* **2010**, *47*, 1916–1923. [CrossRef]
2. Jiang, H.J.; Liang, L.H.; Ma, L.; Guo, J.; Dai, H.L.; Wang, X.G. An analytical solution of three-dimensional steady thermodynamic analysis for a piezoelectric laminated plate using refined plate theory. *Compos. Struct.* **2017**, *162*, 194–209. [CrossRef]
3. He, G.H.; Li, X.W.; Zhong, S.Q.; Zhou, X.; Sheng, X.Z. Weak-form differential quadrature element analysis of plate on a tensionless and frictional foundation using a higher-order kinematics. *Appl. Math. Model.* **2023**, *117*, 87–117. [CrossRef]

4. Lewandowski, R.; Switka, R. Unilateral plate contact with the elastic-plastic Winkler-type foundation. *Comput. Struct.* **1991**, *39*, 641–651. [CrossRef]
5. Winkler, E. *Theory of Elasticity and Strength*; Dominicus: Prague, Czechoslovakia, 1867.
6. Jeong, S.; Kim, Y.; Kim, J. Influence on lateral rigidity of offshore piles using proposed p-y curves. *Ocean Eng.* **2011**, *38*, 397–408. [CrossRef]
7. He, G.; Li, X.; Lou, R. Nonlinear FEA of higher order beam resting on a tensionless foundation with friction. *Geomech. Eng.* **2016**, *11*, 95–116. [CrossRef]
8. Bayat, M.; Andersen, L.V.; Ibsen, L.B. p-y-ẏ curves for dynamic analysis of offshore wind turbine monopile foundations. *Soil Dyn. Earthq. Eng.* **2016**, *90*, 38–51. [CrossRef]
9. Ghorbanpour-Arani, A.H.; Sharafi, M.M.; Kolahchi, R. Nonlocal viscoelasticity based vibration of double viscoelastic piezoelectric nanobeam systems. *Meccanica* **2016**, *51*, 25–40. [CrossRef]
10. Arani, A.G.; Abdollahian, M.; Kolahchi, R. Nonlinear vibration of embedded smart composite microtube conveying fluid based on modified couple stress theory. *Polym. Compos.* **2015**, *36*, 1314–1324. [CrossRef]
11. Kerr, A.D. A study of a new foundation model. *Acta Mech.* **1965**, *1*, 135–147. [CrossRef]
12. Timoshenko, S.P.; Woinowsky-Krieger, S. *Theory of Plates and Shells*; McGraw-Hill: New York, NY, USA, 1959.
13. Mindlin, R.D. Influence of rotary inertia and shear on flexural motions of isotropic elastic plates. *ASME J. Appl. Mech.* **1951**, *18*, 31–38. [CrossRef]
14. Özdemir, Y.I. Using fourth order element for free vibration parametric analysis of thick plates resting on elastic foundation. *Struct. Eng. Mech.* **2018**, *65*, 213–222.
15. Özdemir, Y.I. Dynamic analysis of thick plates resting on Winkler foundation using a new finite element. *Iran. J. Sci. Technol. Trans. Civ. Eng.* **2020**, *44*, 69–79. [CrossRef]
16. Farida, A.F.; Reda, M.; Rashed, Y.F. Efficient analysis of plates on nonlinear foundations. *Eng. Anal. Bound. Elem.* **2017**, *83*, 1–24. [CrossRef]
17. Ragba, O.; Matbulya, M.S.; Civalek, Ö. Free vibration of irregular plates via indirect differential quadrature and singular convolution techniques. *Eng. Anal. Bound. Elem.* **2012**, *128*, 66–79. [CrossRef]
18. Ferreira, A.J.M.; Castro, L.M.S.; Bertoluzza, S. Analysis of plates on Winkler foundation by wavelet collocation. *Meccanica* **2011**, *46*, 865–873. [CrossRef]
19. Yue, F.; Wang, F.; Jia, S.; Wu, Z.; Wang, Z. Bending analysis of circular thin plates resting on elastic foundations using two modified Vlasov models. *Math. Probl. Eng.* **2020**, *2020*, 2345347. [CrossRef]
20. Mohammadimehr, M.; Mehrabi, M.; Afshari, H.; Salemi, M.; Torabi, K. Free vibration and buckling analyses of functionally graded annular thin sector plate in-plane loads using GDQM. *Struct. Eng. Mech.* **2019**, *71*, 525–544.
21. Singh, S.J.; Harsha, S.P. Nonlinear dynamic analysis of sandwich S-FGM plate resting on pasternak foundation under thermal environment. *Eur. J. Mech.-A/Solids* **2019**, *76*, 155–179. [CrossRef]
22. Huang, X.L.; Dong, L.; Wei, G.Z.; Zhong, D.Y. Nonlinear free and forced vibrations of porous sigmoid functionally graded plates on nonlinear elastic foundations. *Compos. Struct.* **2019**, *228*, 111326. [CrossRef]
23. Rachid, A.; Ouinas, D.; Lousdad, A.; Zaoui, F.Z.; Achour, B.; Gasmi, H.; Butt, T.A. A Tounsi Mechanical behavior and free vibration analysis of FG doubly curved shells on elastic foundation via a new modified displacements field model of 2D and quasi-3D HSDTs. *Thin-Walled Struct.* **2021**, *172*, 108783. [CrossRef]
24. Vu, T.-V.; Nguyen, H.T.T.; Nguyen-Van, H.; Nguyen, T.-P.; Curiel-Sosa, J.L. A refined quasi-3D logarithmic shear deformation theory-based effective meshfree method for analysis of functionally graded plates resting on the elastic foundation. *Eng. Anal. Bound. Elem.* **2021**, *131*, 174–193. [CrossRef]
25. Kumar, S.; Jana, P. Accurate solution for free vibration behaviour of stepped FGM plates implementing the dynamic stiffness method. *Structures* **2023**, *45*, 1971–1989. [CrossRef]
26. Reddy, J.N. *Mechanics of Laminated Composite Plates and Shells: Theory and Analysis*; CRC Press: Boca Raton, FL, USA, 2003.
27. Yan, Z.D. *Fourier Series Solution Method in Structural Mechanics*; Tianjin University Press: Tianjin, China, 1989. (In Chinese)
28. Wang, C.L. Study on Theory of Elastic Half-Space for Soli-Foundation Dynamic Interaction. Master's Thesis, Xi'an University of Architecture and Technology, Xi'an, China, 2006. (In Chinese).
29. Li, R.; Zhong, Y.; Li, M. Analytic bending solutions of free rectangular thin plates resting on elastic foundations by a new symplectic superposition method. *Proc. R. Soc.* **2013**, *A469*, 20120681. [CrossRef]
30. Bai, E.; Zhang, C.; Chen, A.; Su, X. Analytical solution of the bending problem of free orthotropic rectangular thin plate on two-parameter elastic foundation. *J. Appl. Math. Mech.* **2021**, *101*, e202000358. [CrossRef]
31. Tenenbaum, J.; Eisenberger, M. Analytic solution for buckling of rectangular isotropic plates with internal point supports. *Thin Wall Struct.* **2023**, *163*, 107640. [CrossRef]
32. Feldman, E.; Aboudi, J. Buckling analysis of functionally graded plates subjected to uniaxial loading. *Compos. Struct.* **1997**, *38*, 29–36. [CrossRef]
33. Yang, W.; Zhang, W.; Wang, X.; Lu, G. Nonlinear delamination buckling and expansion of functionally graded laminated piezoelectric composite shells. *Int. J. Solids Struct.* **2014**, *51*, 894–903. [CrossRef]

34. Duc, N.C.; Cong, P.H.; Tuan, N.D.; Tran, P.; Anh, V.M.; Quang, V.D. Nonlinear thermoelectro-mechanical dynamic response of shear deformable piezoelectric sigmoid functionally graded sandwich circular cylindrical shells on elastic foundations. *J. Sandw. Struct. Mater.* **2016**, *18*, 445–473. [CrossRef]
35. Duc, N.D. Nonlinear thermal dynamic analysis of eccentrically stiffened S-FGM circular cylindrical shells surrounded on elastic foundations using the Reddy's third-order shear deformation shell theory. *Eur. J. Mech.-A/Solids* **2016**, *58*, 10. [CrossRef]
36. Lee, Y.; Zhao, X.; Reddy, J. Postbuckling analysis of functionally graded plates subject to compressive and thermal loads. *Comput. Methods Appl. Mech. Eng.* **2010**, *199*, 1645–1653. [CrossRef]
37. Tung, H.V. Postbuckling behavior of functionally graded cylindrical panels with tangential edge constraints and resting on elastic foundations. *Compos. Struct.* **2013**, *100*, 532–541. [CrossRef]
38. Ozturk, A.; Gulgec, M. Elastic–plastic stress analysis in a long functionally graded solid cylinder with fixed ends subjected to uniform heat generation. *Int. J. Eng. Sci.* **2011**, *49*, 1047–1061. [CrossRef]
39. Eqlima, M.; Ali, G.; Akbari, A.R. Elastic-plastic analysis of functionally graded rotating disks with variable thickness and temperature-dependent material properties under mechanical loading and unloading. *Aerosp. Sci. Technol.* **2016**, *59*, 57–68.
40. Sladek, J.; Sladek, V.; Repka, M. Evaluation of the T-stress for cracks in functionally graded materials by the FEM. *Theoret. Appl. Fract. Mech.* **2016**, *86*, 332–341. [CrossRef]